

UNIVERSITY OF HOUSTON

DEPARTMENT OF PHYSICS

FINAL PROGRESS REPORT

September 1, 1967 - February 29, 1968

SPACE RELATED SCIENTIFIC  
AND TECHNICAL INVESTIGATIONS

GPO PRICE \$ \_\_\_\_\_

CFSTI PRICE(S) \$ \_\_\_\_\_

Hard copy (HC) 3.50

Microfiche (MF) 65

ff 653 July 65

NASA GRANT 44-005-022

OFFICE OF GRANTS & RESEARCH CONTRACTS

NASA - OSSA



May 1968

John W. Kern

N68-25369  
(ACCESSION NUMBER)  
44  
(PAGES)  
Or #94778  
(NASA CR OR TAX OR AD NUMBER)

(THRU)  
(CODE)  
(CATEGORY)

FACILITY FORM 602

The investigation program during the past six month period has yielded significant results in a number of areas. The program is divided into five areas: 1) Low Temperature Physics, 2) Solid State Physics, 3) Atomic Physics, 4) Comet Physics, and 5) Physics of Space Related Flow Problems. The research results in these areas are described in detail below. The investigations have been carried out in close collaboration with scientists at the NASA Manned Spacecraft Center, Houston. The results and the capabilities of the investigators named in this report are continually available for application to current operational programs of NASA-MSC. The contacts and communications opened by this research will continue to be maintained. A supplement to this grant has been approved for next year, enabling the extension of the work on 1) Low Temperature Physics, 2) Atomic Physics, 3) Space Related Flows and 4) Plasma Physics. The last area is new, and reflects a significant addition to the scientific and technical capabilities of the Department of Physics of the University of Houston during the past year. Professor Melvin Eisner and Dr. Gregory Haas have joined our faculty, bringing an exceptional experimental capability in Plasma Physics to this area.

The investigations for the past year have yielded to date seven M.S. theses and one Ph.D. thesis. Work currently in progress on the present grant will yield three M.S. theses and four Ph.D. theses. New research initiated under the supplementary grant is expected to generate a similar output of trained graduates. All of the research results have been presented as papers at meetings of professional societies whenever appropriate. Many of the research topics outlined below are in various stages of submission for publication. It is the policy of the Department of Physics to expedite publication of research results whenever they are of substantive or topical nature. Publication of some results may be deferred until completion of a specific program. We review the program content of grant-funded research periodically to ensure the quality and relevance of work being supported under individual grants. This is ensured by early submission of work for publication and scientific scrutiny. Some technical programs do not yield material of publishable nature. Such programs are subjected to the continuing review of interested personnel at NASA-MSC in connection with development of programs at that center. Current publications associated with this contract include a translation of E. Cartan's Lectures on Integral Invariants, by J. Pierce and R. M. Kiehn; R. M. Kiehn, "Poincare Stresses and Mach's Principle," Bull. A.P.S. 11, 773, 1966; A. F. Hildebrandt and H. E. Corke, "Pressure Studies of Pure Superfluid Flow", Phys. Fluids 155, March 1968; N. S. Kovar and R. P. Kovar, "Optical Pumping and the D Line

Ratio of Comet 1962 III", Solar Physics, April 1968; J. W. Kern and C. L. Semar, "Solar-Wind Termination and the Interstellar Medium", Trans. Am. Geophys. Union 49, 263-264, 1968. It is expected that the current results will yield a significant number of additional papers. Available reprints of papers reporting investigations supported under this contract will be forwarded with the semiannual reports for the supplementary grant.

The following is, then, a more detailed summary of work done under the current contract. For each research project, a separate report is given which indicates the work done, the results obtained, degrees earned by graduate students involved, the work remaining to be done, and, where appropriate, the status of the publication resulting from the work.

Questions regarding the work described in this grant may be directed to Dr. John W. Kern, Chairman, Department of Physics, University of Houston, Houston, Texas 77004, (713) 748-6600, Extension 691. The investigators named in the body of the report may be contacted individually regarding their work at the same address.

1. Low Temperature Physics, Dr. Alvin F. Hildebrandt, Associate Professor of Physics.

a) Second Sound in a Moving Coordinate System. Earl M. Johnson and A. F. Hildebrandt.

An unusual property displayed by liquid helium below 2.17°K, is the ability of helium II to conduct heat in the form of a wave motion of superfluid rather than the usual processes such as diffusion and convection. Tiza<sup>(1)</sup> predicted this property as a consequence of his version of a two-fluid theory. He noted that if the two fluids were present together and if the coupling between them was small, then the two fluids should be able to oscillate out of phase with each other. This oscillation would be subject to the condition of no net flow of mass, that is  $\rho_n \vec{v}_n + \rho_s \vec{v}_s = 0$ , where  $\vec{v}_n$  and  $\vec{v}_s$  are the velocities of the normal and superfluid components respectively. The above conditions represent a progressive wave motion in which alternate regions of the liquid exhibit an excess and defect of entropy and constitute a temperature wave. These waves differ from ordinary sound in which the fluids move in phase and the excess and defect is one of pressure. Landau's<sup>(2)</sup> theory of liquid helium II also predicted temperature waves to which he gave the name "second sound".

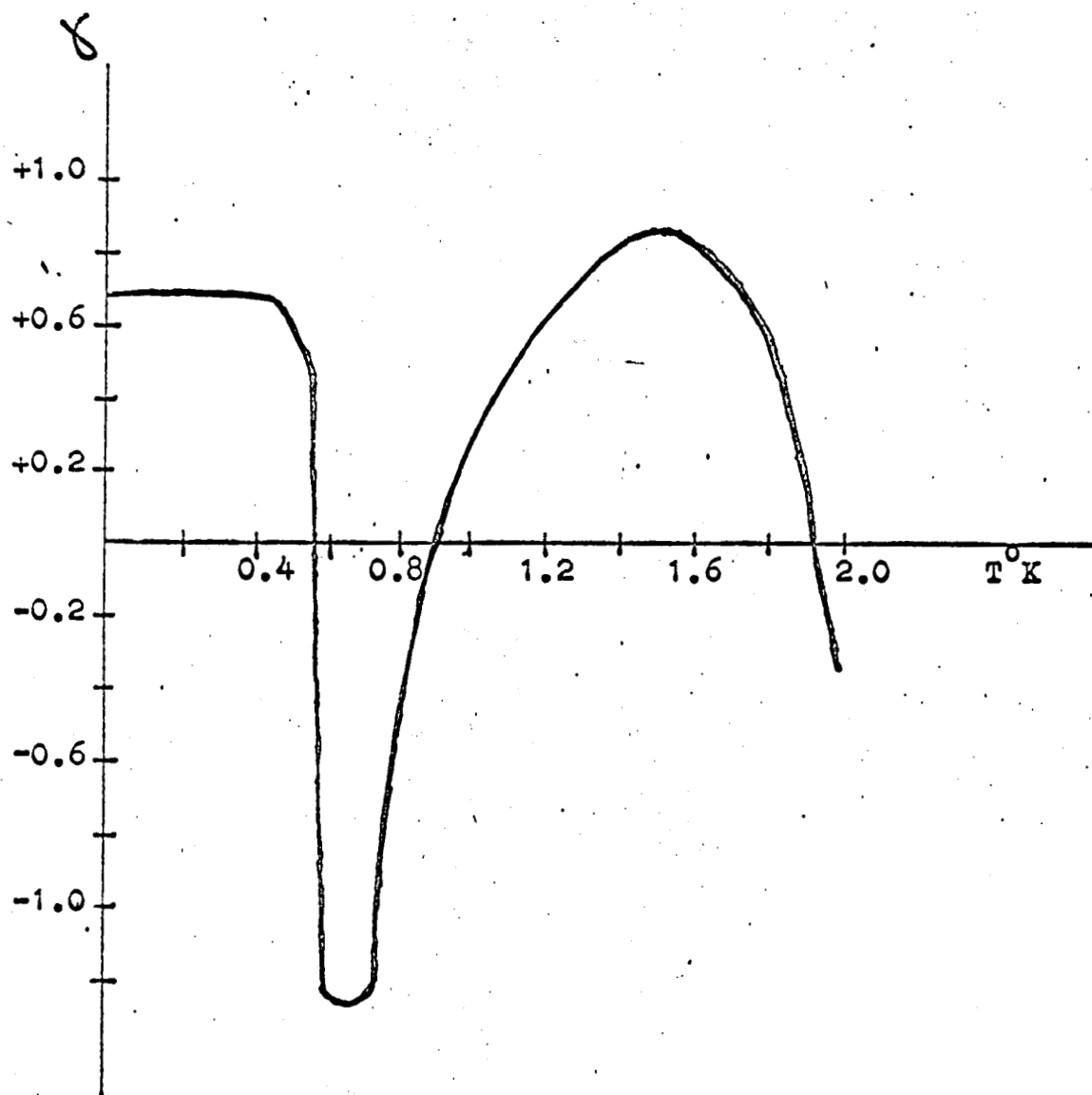
From ordinary hydrodynamics it is known that an "entrainment" of sound occurs in a moving fluid. A similar effect is expected to take place in the hydrodynamics of helium II. The "entrainment" of second sound in counter flowing superfluid and normal fluid is expected, according to theory<sup>(3)</sup>, to be a complicated function of temperature. The velocity of second sound in counter flowing superfluid and normal fluid is given by the expression

$$u_2 = c_2 + \gamma v_n \quad (1)$$

where  $c_2$  is the velocity of second sound in stationary helium II,  $v_n$  is the velocity of the normal fluid component and  $\gamma$  is the entrainment coefficient. The dependance of  $\gamma$  on temperature is shown in figure (1).

In order to verify Khalatnikov's theory<sup>(3)</sup> it is necessary to study the effective time of flight of a second sound pulse in the presence of a thermal current, (counter flowing superfluid and normal fluid).

If we consider the time of flight of a second sound pulse in stationary helium II we have  $t_1 = x/c_2$ , where  $x$  is the distance between the second sound transmitter and receiver and  $c_2$  is the velocity of



"ENTRAINMENT" COEFFICIENT

FIGURE (1)

second sound in stationary helium II. Now if we measure the time of flight of a second sound pulse with a thermal current present we have  $t_2 = x/\mu$ , where  $\mu$  is given by equation (1),  $\mu = c_2 + \gamma v_n$ . The difference,  $t_1 - t_2$ , will be the change in the time of flight due to the "entrainment" of second sound in moving helium II.

A measurement has been made of the change in time of flight of a second sound pulse as a function of the relative velocity ( $\vec{v}_n - \vec{v}_s$ ), where  $\vec{v}_n$  is the normal fluid velocity and  $\vec{v}_s$  is the superfluid velocity. From this measurement we may infer how the reference frame of second sound varies with the motion of the normal fluid and the superfluid. The change in time of flight was measured within  $\pm 0.14 \times 10^{-6}$  seconds.

The chief problem encountered was the accurate measurement of the change in the time of flight of a second sound pulse as a function of counter flowing superfluid and normal fluid for small velocities. If we calculate the change of the time of flight of a second sound pulse at a temperature of  $1.43^\circ\text{K}$  and a normal fluid velocity of  $0.5 \text{ cm/sec}$  we obtain a value of  $1.2 \text{ microseconds}$  from theory<sup>(3)</sup>. The distance between the second sound transmitter and receiver being  $10 \text{ cm}$ .

Two problems were encountered. First, the velocity of second sound is a strong function of temperature and the second is the profile of the received second sound pulse as a function of the power input to the second sound transmitter. Also it has been shown theoretically by Temperley<sup>(4)</sup> and Khalatnikov<sup>(5)</sup> and experimentally verified by Dessler and Fairbank<sup>(6)</sup> that nonlinear effects are present.

A second sound pulse was constrained to propagate in a second sound cell, figure (2). The second sound cell consisted of a brass tube of  $3/8$  inch inner diameter,  $1$  inch outer diameter and a length of  $3.937$  inches, the total length being  $7.5$  inches. In the  $7/8$  inner diameter portion of the second sound cell a heater of  $105 \pm 0.1\%$  ohms and a second sound transmitter made of I.R.C. resistance strips were placed. After the heater and transmitter were installed the end of the brass tube was sealed by soft soldering a brass disc in place at the end of this portion of the second sound cell. Four stubakopffs were inserted in the walls of the brass tube to make electrical contact with the transmitter and heater. As this portion of the second sound cell was sealed the only opening to the liquid helium II bath was at the  $3/8$  inch opening at the other end of the second sound cell. At the open end of the second sound cell a second sound receiver was placed. Both transmitter and receiver were a fixed distance with respect to each other. The transmitter consisted of a thin layer of carbon on a phenolic backing, electrical contact was made with silver paint electrodes. The transmitter was made square as to provide a uniform heat flow density through the whole wave front. The resistance of the transmitter at room temperature was approximately  $50 \text{ ohms per square}$  and approximately  $200 \text{ ohms per square}$  at  $1.5^\circ\text{K}$ . The second sound receiver was constructed by painting

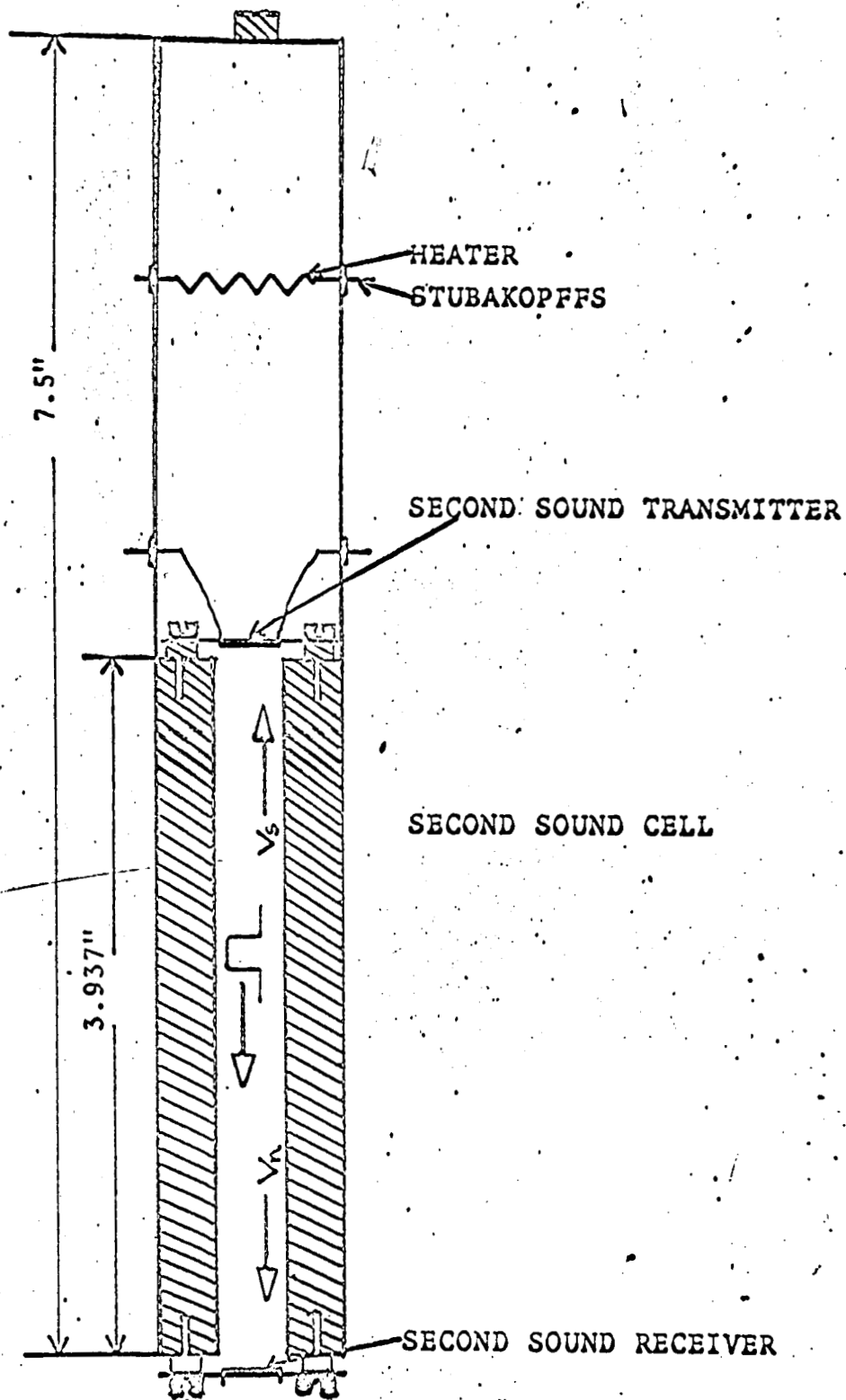


FIGURE (2)

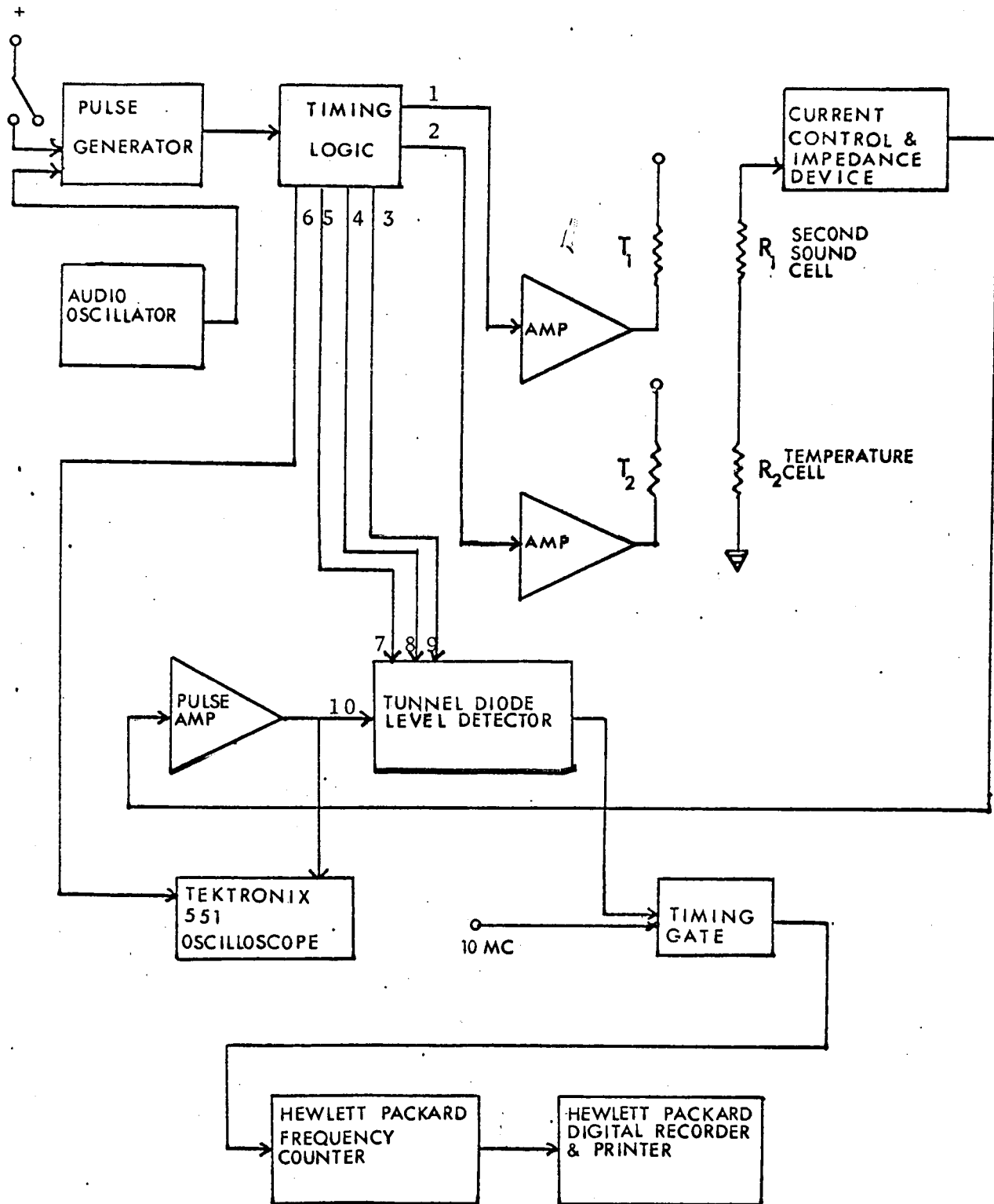
an aquadag layer on a square phenolic backing. Several coats had to be applied before the proper resistance value was obtained. At room temperature the resistance was approximately 100 to 1000 ohms per square depending on how many coats of aquadag were applied to the phenolic backing. Because of the negative temperature coefficient of aquadag the resistance would increase as the temperature was lowered. The temperature coefficient was found to be approximately 1000 ohms per degree.

During measurements of the time of flight of the second sound pulse, the second sound cell was completely submerged in the liquid helium II bath. The temperature was determined from the vapor pressure of the bath, measured by a Wallace and Tiernan Absolute Pressure gauge. The high thermal conductivity of helium II assured that the temperature inside the second sound cell was very close to that of the ambient bath.

The electronic system used in this experiment is represented in figure (3) by a block diagram. A square pulse was generated from a pulse generator that consisted of a R-S flip-flop circuit and a variable monostable circuit. The R-S flip-flop was triggered by a manual switch or a Schmidt trigger circuit which was driven by a variable frequency audio oscillator. Figure (4) is a schematic of the pulse generator circuit. By changing the frequency of the audio oscillator the repetition rate of the pulse was varied. Continuous second sound pulses were used only to check the electronics during the experiment. The function of the variable monostable was to vary the pulse width. The pulse produced by the pulse generator had a rise time of 40 nanoseconds and a variable width of 10 microseconds to 160 microseconds. The pulse was then fed into a timing logic network. The timing logic network had six different outputs, labeled 1,2,3,4,5, and 6 in figure (3). Figure (5) is a schematic of the timing logic network.

Output 1 of the timing logic network produced a negative square pulse which was fed into power amplifier A. Figure (6) is a schematic of power amplifier A which is similar to power amplifier B represented in figure (3). The output of power amplifier A was connected via a coaxial cable to a second sound transmitter  $T_1$  located in the second sound cell which was located in the helium II bath. Output 6 of the timing logic network produced a positive square pulse which was fed into the external trigger input of a Tektronic 551 Dual-Beam oscilloscope.

Receiver  $R_1$  was connected in series by a coaxial cable to a constant current control device and impedance matching device. A d.c. bias current of approximately one milliamperere was passed through receiver  $R_1$ . The resistance of  $R_1$  changed as the second sound pulse



ELECTRONIC SYSTEM

FIGURE (3)

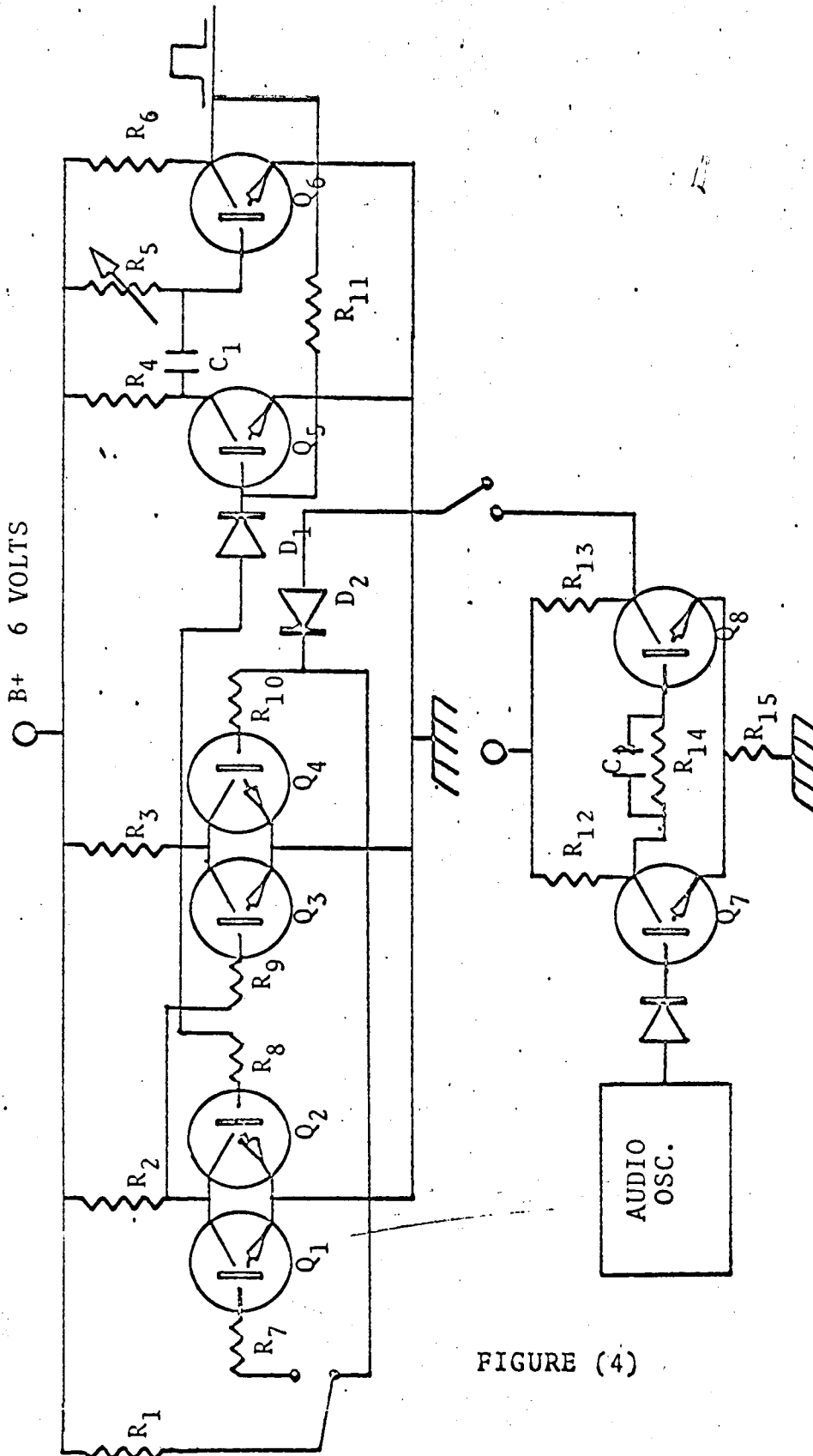
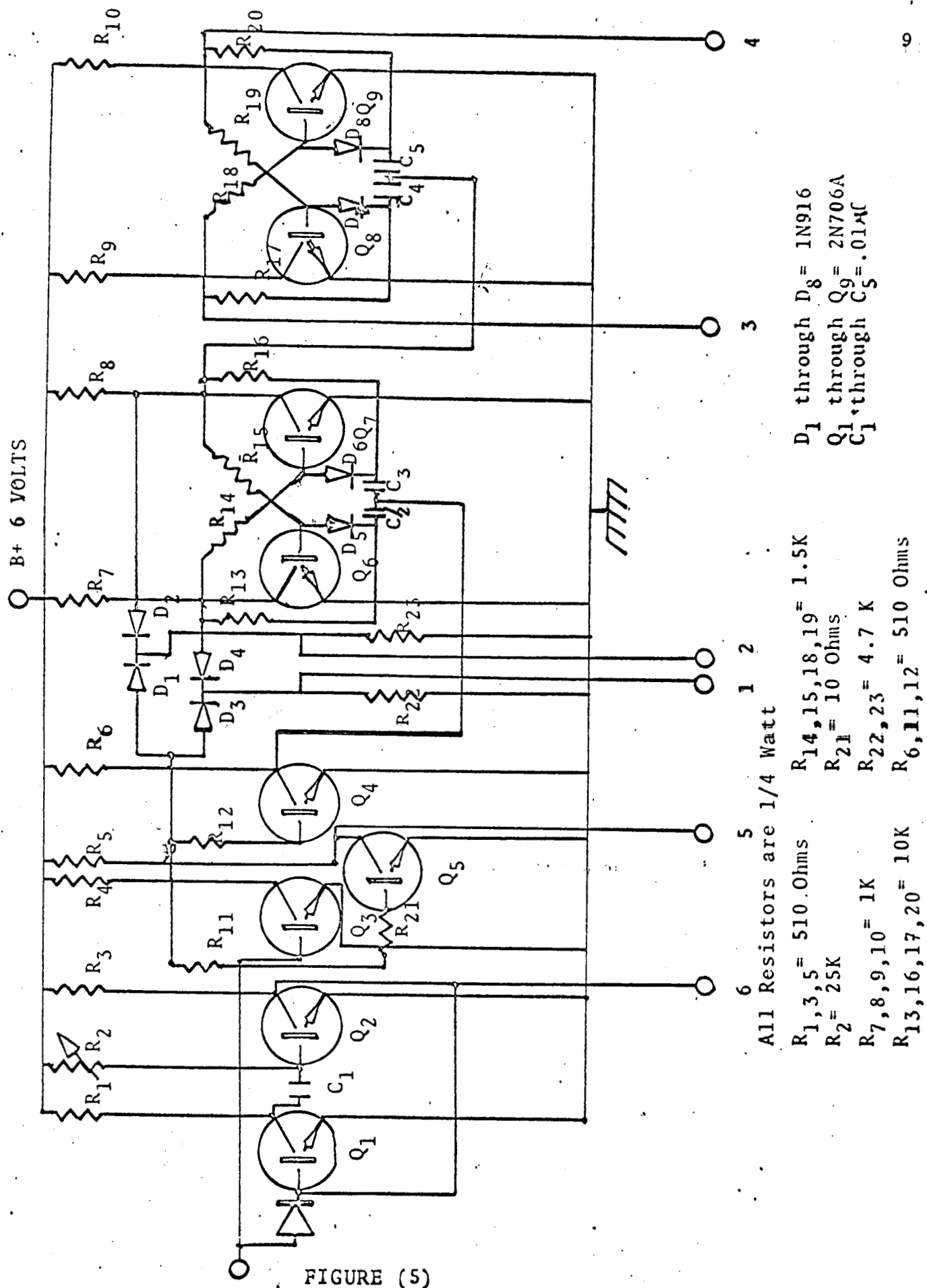


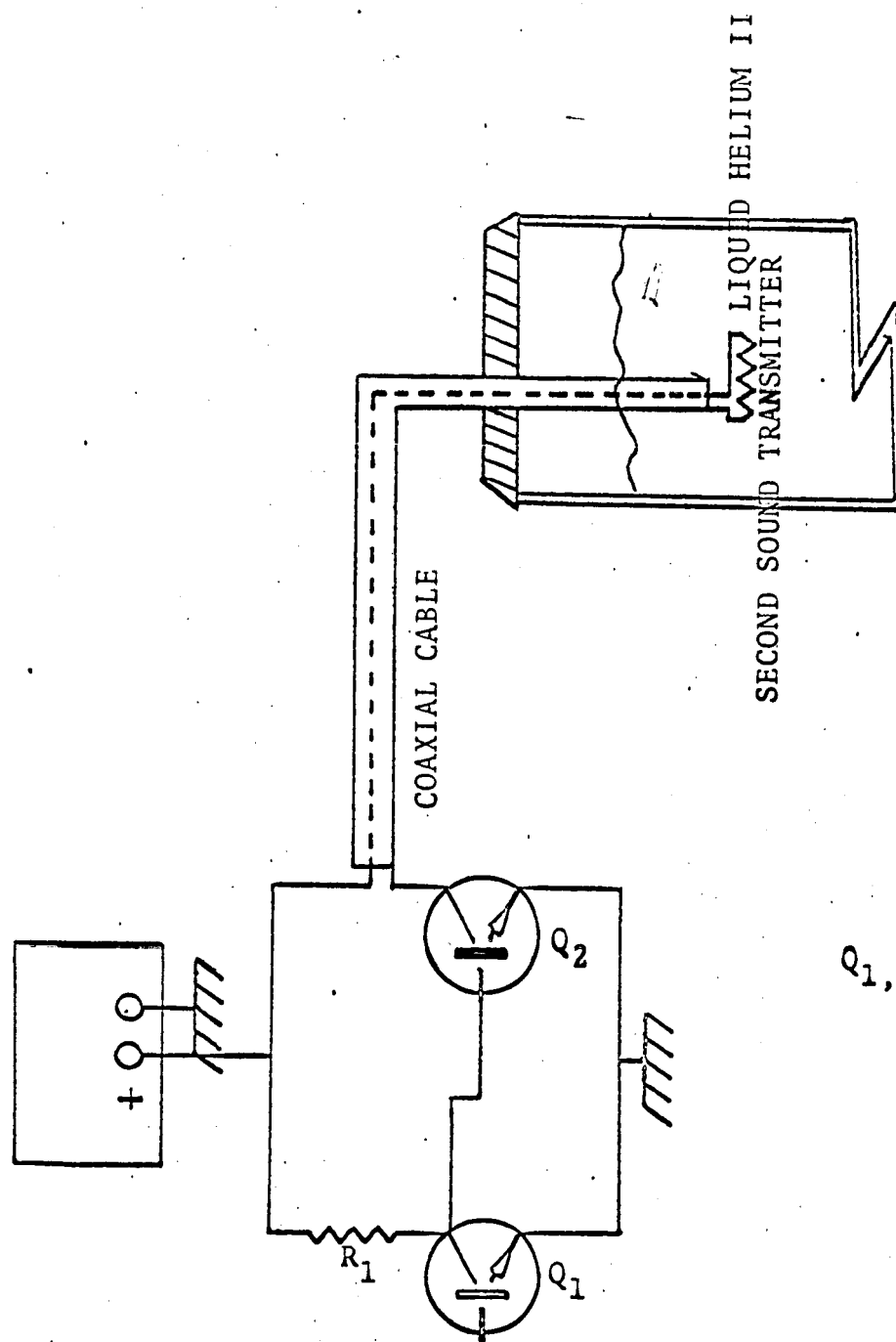
FIGURE (4)

- $R_1 = 2K$  All Resistors are 1/4 Watt  
 $R_2, 3, 4, 6, 12, 13 = 510 \text{ Ohms}$   
 $R_5 = 100K$   
 $R_7, 14 = 6.8K$   
 $R_8, 9, 10 = 220 \text{ Ohms}$   
 $R_{11} = 10K$   
 $R_{15} = 100 \text{ Ohms}$
- $C_1 = .2 \text{ f}$   
 $C_2 = 1.3 \text{ f}$
- $Q_1$  through  $Q_8 = 2N706A$



All Resistors are 1/4 Watt

R<sub>1,3,5</sub> = 510 Ohms  
 R<sub>2</sub> = 25K  
 R<sub>7,8,9,10</sub> = 1K  
 R<sub>13,16,17,20</sub> = 10K  
 R<sub>14,15,18,19</sub> = 1.5K  
 R<sub>21</sub> = 10 Ohms  
 R<sub>22,23</sub> = 4.7 K  
 R<sub>6,11,12</sub> = 510 Ohms



$Q_1, Q_2 = 2N2369A$   
 $R_1 = 47 \text{ ohms, } 1/4\text{Watt}$

FIGURE (6)

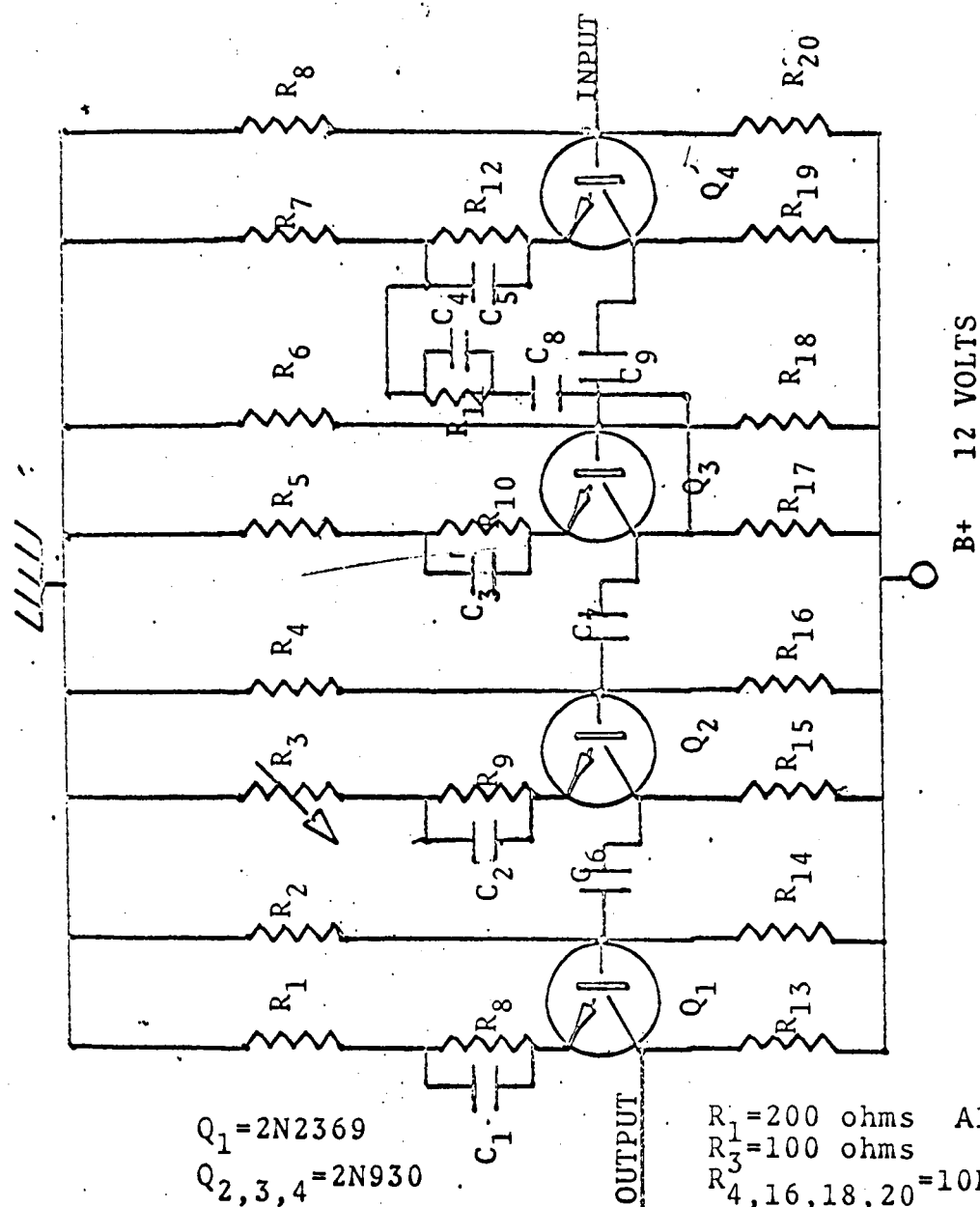
impinging upon the surface of  $R_1$  producing a change in voltage across  $R_1$ . This change in voltage was fed through the constant current and impedance matching device into a pulse amplifier. Figure (7) is a schematic of the pulse amplifier. The output of the pulse amplifier was fed into input 10 of the tunnel diode level detector.

The tunnel diode level detector was utilized to detect the relative time of arrival of the second sound pulse to a high degree of accuracy and reproducibility. A tunnel diode will switch its state in less than one nanosecond when a signal voltage of a few millivolts is received. Figure (8) is a schematic of the tunnel diode level detector system. When the tunnel diode is biased in its low voltage or high current state it can be switched to a high voltage or low current state by a signal voltage which exceeds a preselected trigger level. The trigger level was determined by the low voltage state bias which was accomplished by adjusting the variable resistor  $R_7$ . A pulse from the timing logic was fed into the tunnel diode level detector at pin 9 which reset the tunnel diode into a low voltage state. The received second sound pulse signal then triggered the tunnel diode level detector to a high voltage state. Thus, a voltage pulse was produced whose width was proportional to the time of flight of the second sound pulse. The tunnel diode voltage pulse was then amplified by transistors  $Q_6$  and  $Q_7$  to open the timing gate in figure (9). While the timing gate was open a 10 megacycle signal was counted by a Hewlett Packard 5245L frequency counter. An individual time of flight was measured to within  $\pm 0.1$  microsecond. An output from the frequency counter was fed into a Hewlett Packard Digital Recorder R50-562A. The digital recorder printed out each time of flight of the second sound pulse that was recorded on the frequency counter.

Figures (10), (11), (12), and (13) are graphs of the change in the time of flight of a second sound pulse as a function of the normal fluid velocity. It should be noted that the change in time of flight is implicitly a function of the superfluid velocity, equation (1).

In figure (11) it is not understood why this data is not in good agreement with theory. It was considered that the best possible data would be at the temperature  $1.65^\circ\text{K}$  since the velocity of second sound is least sensitive to temperature changes. Also in Khalanitikov's theory this temperature seems a logical temperature to measure the change in the time of flight of a second sound pulse as a function of counter-flowing superfluid and normal fluid.

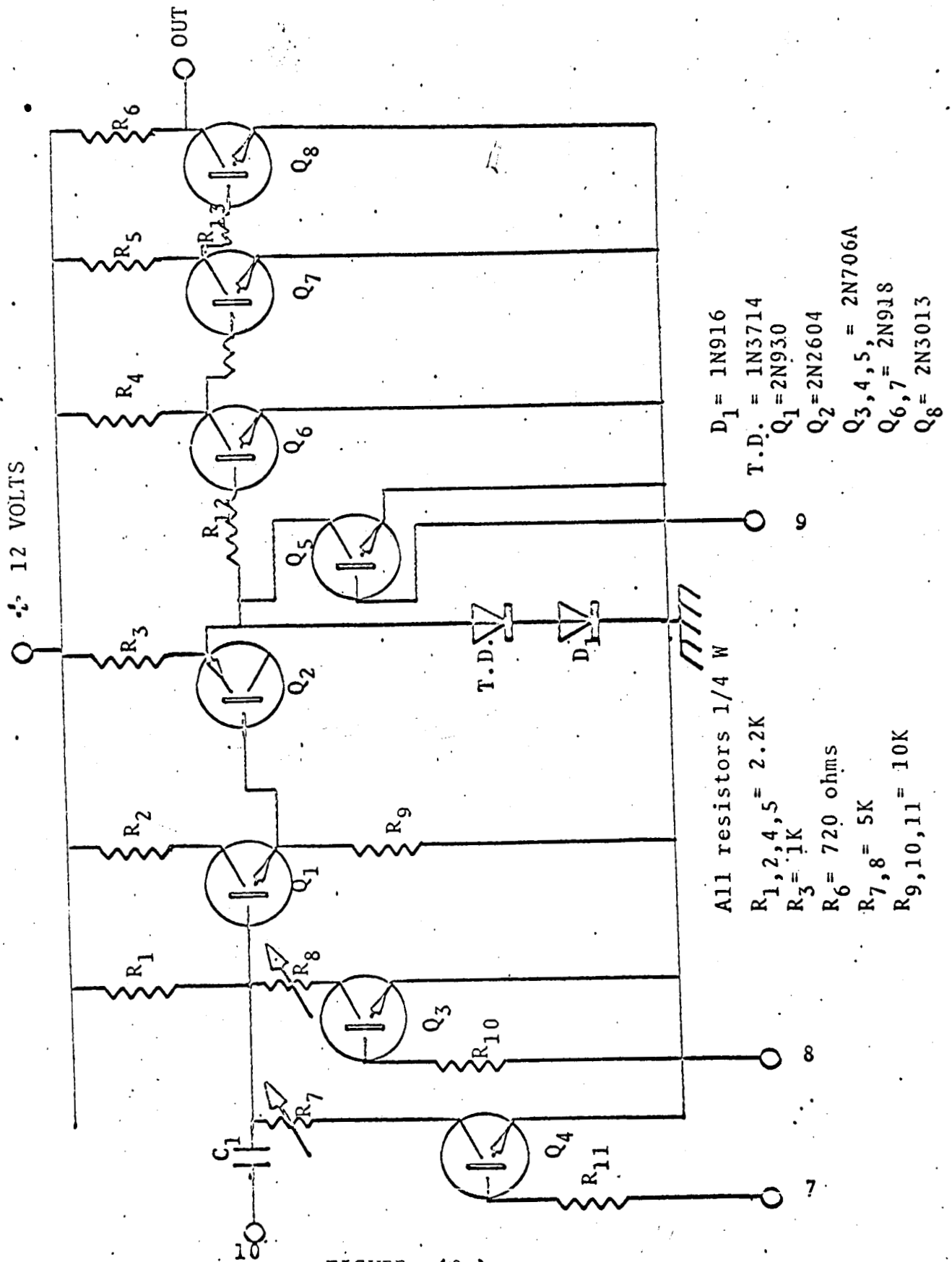
Figure (14) is a composite of the graphs of the change in the time of flight as a function of the normal fluid velocity. The data point at the temperature of  $1.65^\circ\text{K}$  consist of only the first four data points taken. Each data point is composed of 300 to 400 changes in the time of flight of a second sound pulse.

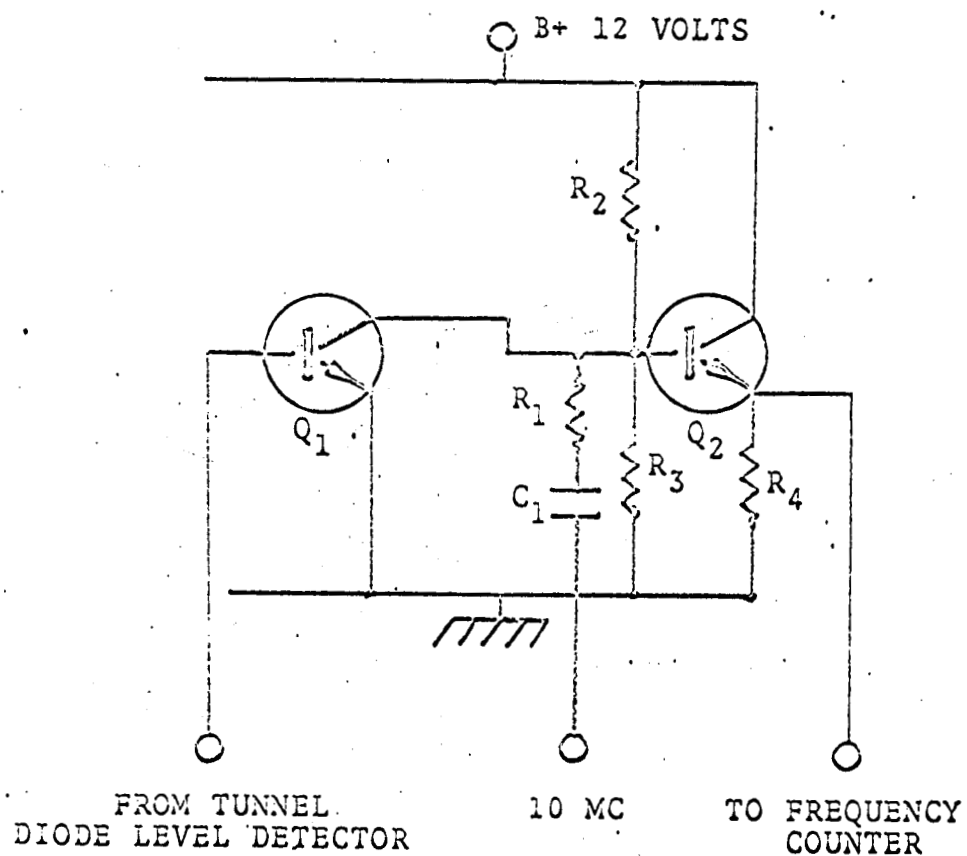


R<sub>1</sub>=200 ohms All resistors, 1/4 W  
 R<sub>3</sub>=100 ohms  
 R<sub>4,16,18,20</sub>=10K  
 R<sub>5,7</sub>=110 ohms  
 R<sub>6,15,17,19</sub>=1K  
 R<sub>9,10,11,12</sub>=105 ohms  
 R<sub>13,14</sub>=51K

C<sub>1</sub>=39μF  
 C<sub>2</sub>=3.4μF  
 C<sub>3,4,5,6</sub>=56μF  
 C<sub>8</sub>=24μF  
 C<sub>9</sub>=10μF

FIGURE (7)





$$R_1 = 2K$$

$$R_2 = 3.3K$$

$$R_3 = 2.2K$$

$$R_4 = 50 \text{ OHMS}$$

$$C_1 = .01 \mu F$$

$$Q_1 = Q_2 = 2N706A$$

FIGURE ( 9 )

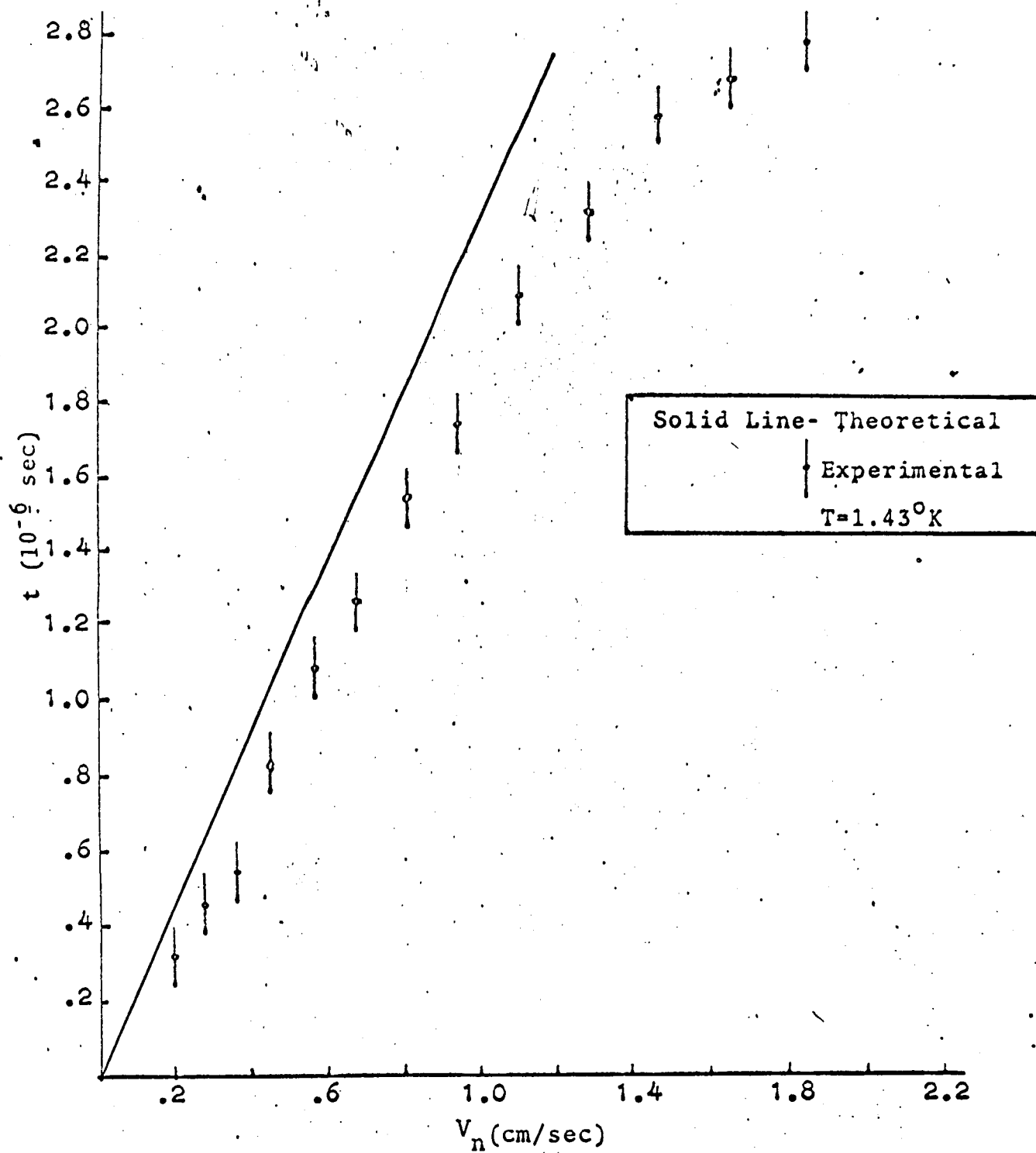


FIGURE (10)

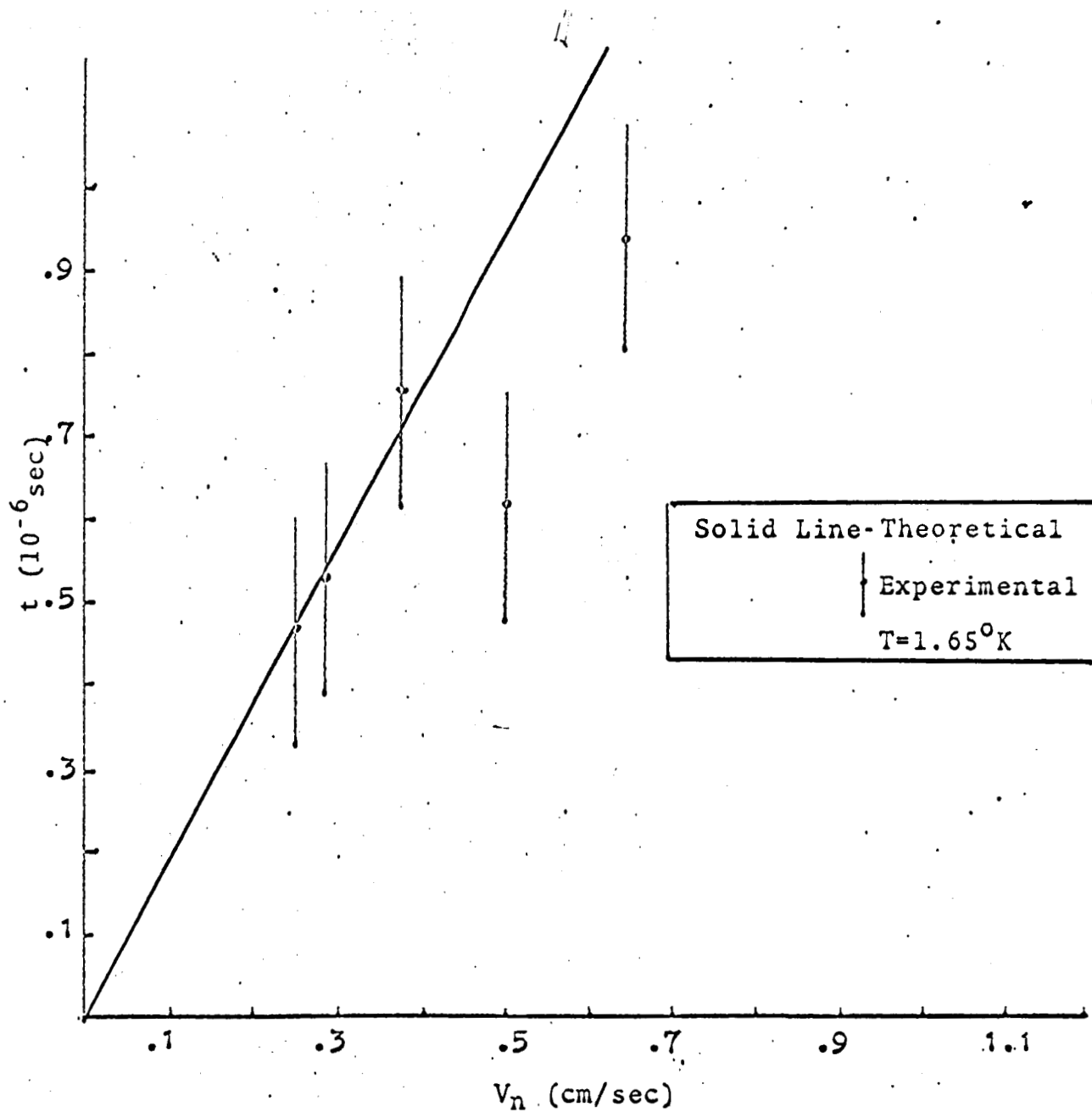


FIGURE (11)

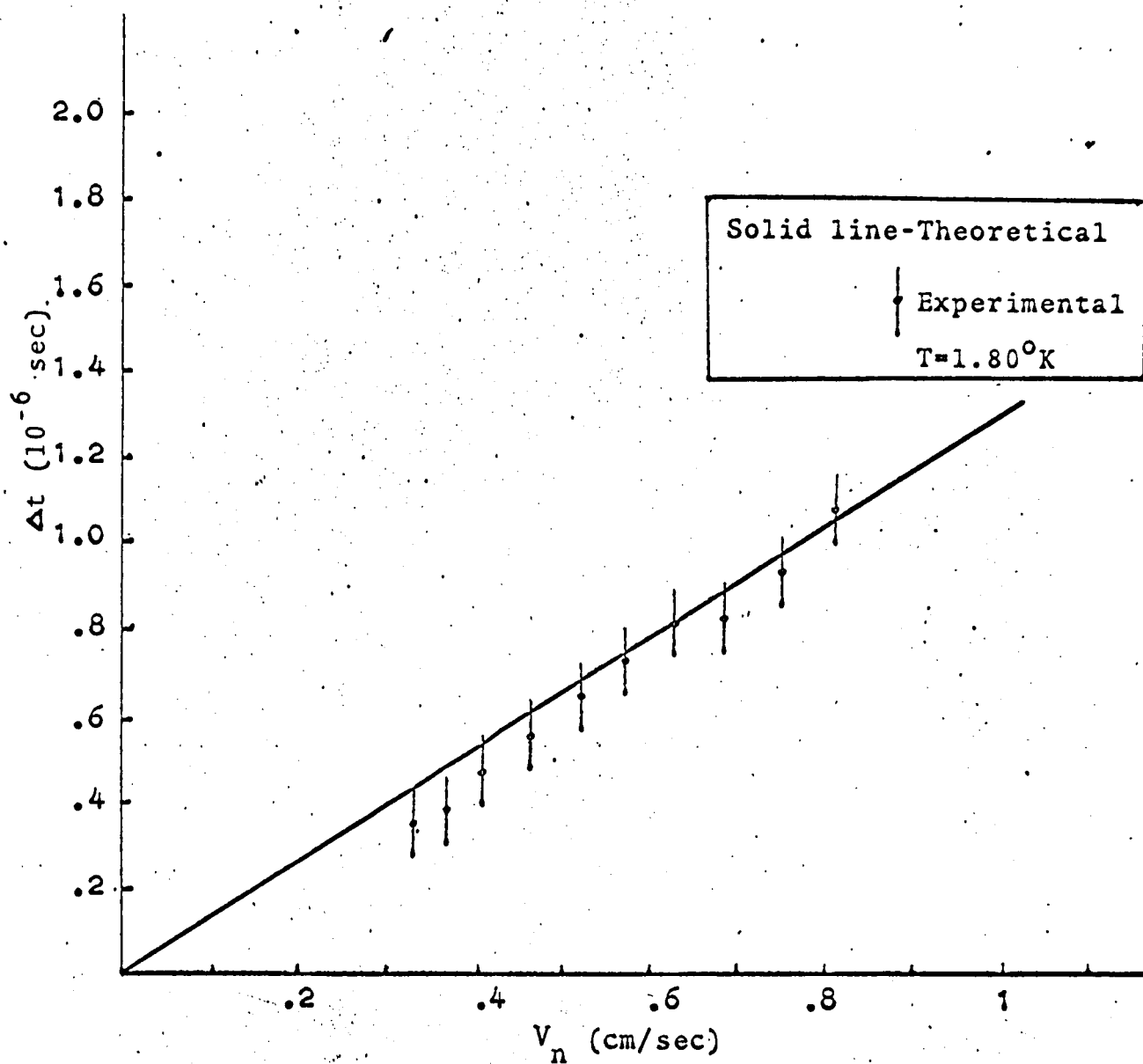


FIGURE (12)

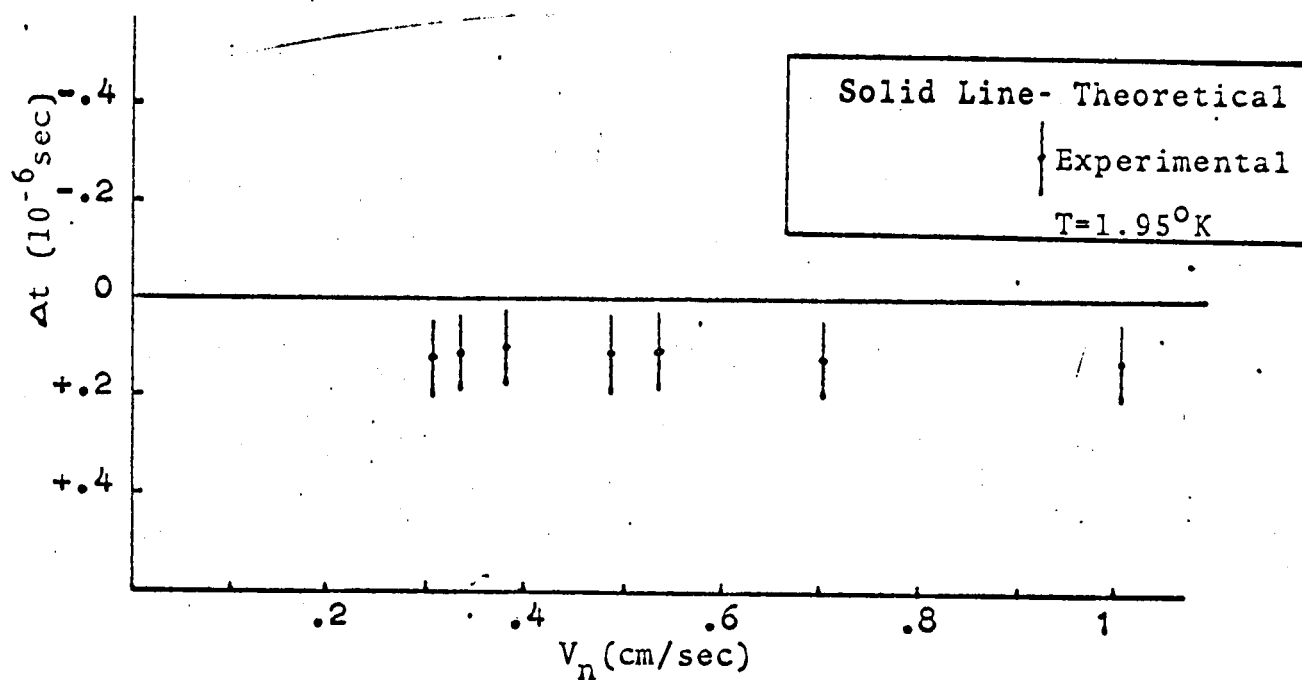


FIGURE (13)

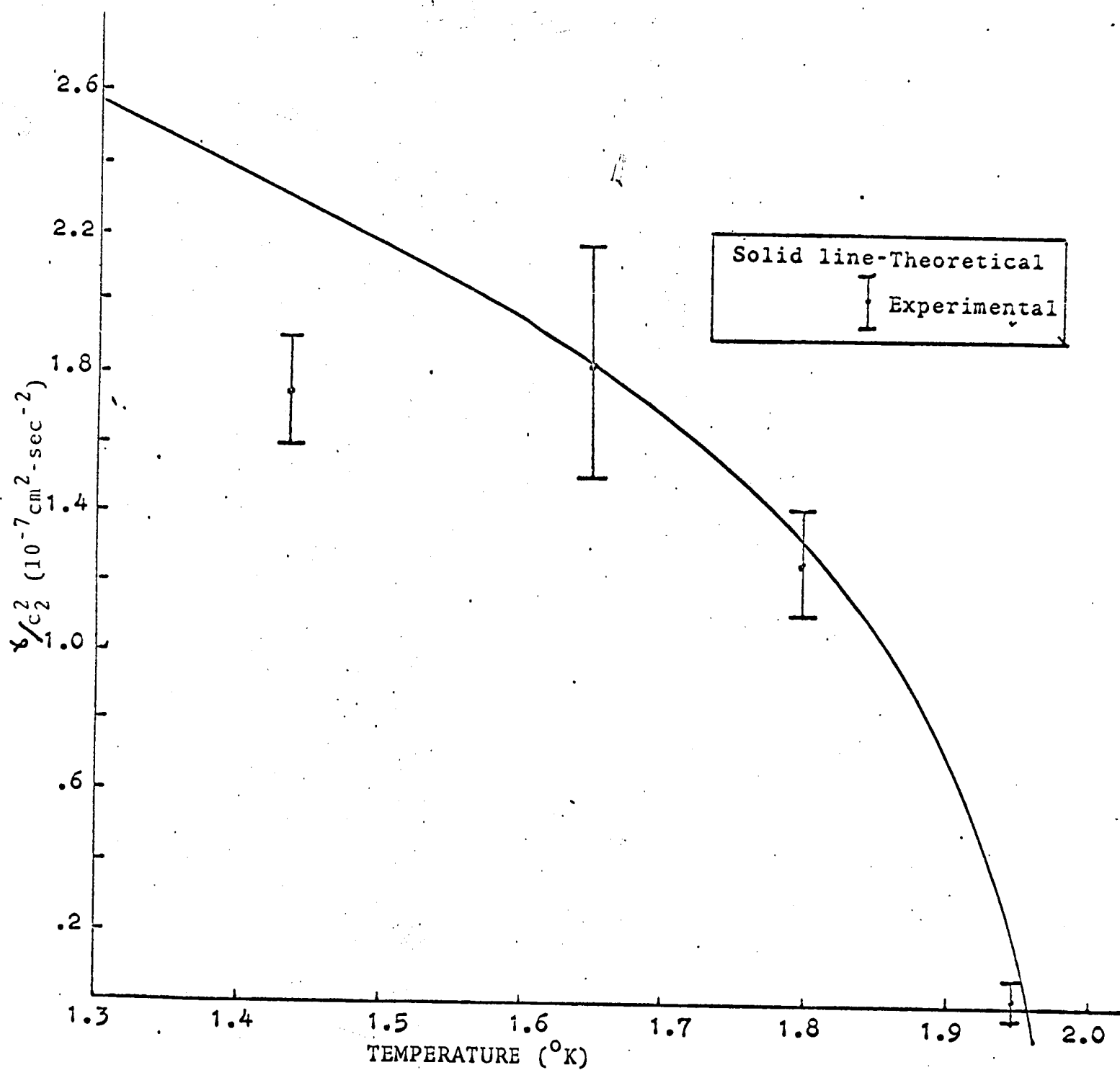


FIGURE (14)

All data taken are in agreement both qualitatively and quantitatively with Khalatnikov's theory<sup>(3)</sup>.

From this data it is possible to infer that the velocity of second sound is relative to both the superfluid and normal fluid components.

From the fact that the entrainment coefficient,  $\gamma$ , in Khalatnikov's theory changes sign at several temperatures, figure (1), it follows that the "entrainment" of the second sound can take place whether in the direction of the thermal current or in the opposite direction to the thermal current. To observe this effect we would need to cover the temperature range from 1.0°K down to 0.1°K. A measurement of the change in the time of flight of a second sound pulse as a function of the superfluid velocity alone can be accomplished by clamping the normal fluid.

A long standing problem in superfluid physics is the question: Can helium II be made to rotate as a whole or does the superfluid component remain at rest and the normal fluid rotate<sup>(7)</sup>? R.G. Wheeler, C. H. Blackwood and C. T. Lane<sup>(8)</sup> have reported that the time of flight of a second sound pulse is constant in rotating helium II. The results of the above experiment indicates the time of flight of second sound should also change in a rotating coordinate system if indeed the fluid rotates. This proposed experiment will permit investigation of the proposed irrotational nature of the superfluid velocity. Using the pulse technique this investigation can be carried out. The experimental rotational apparatus has already been developed from previous designs<sup>(9)</sup>.

Because second sound of superfluid helium obeys a scalar theory, it has been argued that the velocity of second sound would be unaffected by rotation. From the results of the linear flow of the normal component of helium II the velocity of second sound does change. From this we infer that the time of flight of a second sound pulse should also change in a rotating coordinate system if, indeed, the fluid rotates. This will permit experimental investigation of the proposed curless nature of the superfluid velocity.

The linear flow research has been approved for a M.S. thesis and a manuscript is being prepared for publication.

b) Pressure Measurement in Superfluid Helium Flow. H. E. Corke and A. F. Hildebrandt.

The results of this work has been published in Physics of Fluids, 11, 155, March 1968. A copy of the published paper is attached.

c) Quantization of Vortices in Simply and Doubly Connected Superfluid Regions, Thomas N. C. Tsien and Alvin F. Hildebrandt.

The quantization of superfluid about a spinning rod is being studied. Evidence of quantized circulation can be illustrated by a very accurate determination of superfluid flow past the rod using capacitance techniques developed by Corke and Hildebrandt in the previous report. A cylindrical coaxial capacitance has been designed as a level sensor capable of detecting superfluid level changes of  $10^{-5}$  cm. The level sensor requires an up-down counter which has been purchased by the University. The rotating apparatus and associated electronics has been designed and is being assembled.

References

- (1) L. Tiza, Nature, 141, 913 (1938).
- (2) L. Landau, J. Phys. (U.S.S.R.), 5, 71 (1941).
- (3) I. M. Khalatnikov, J. Exptl. Theoret. Phys. (U.S.S.R.) 30, 617-619 (Mar. 1956).
- (4) H. N. V. Temperley, Proc. Phys. Soc. (London), A64, 105 (1951).
- (5) I. M. Khalatnikov, Doklady Acad. Nauk., (U.S.S.R.) 79, No. 2 (1952).
- (6) A. J. Dessler and W. M. Fairbank, Phys. Rev. 104, 6 (1956).
- (7) F. London, Superfluids (John Wiley & Sons, Inc., New York, 1954), Vol. II.
- (8) R. G. Wheeler, C. H. Blackwood and C. T. Lane, Phys. Rev. 99, 1667 (1955).
- (9) A. F. Hildebrandt, Phys. Rev. Letters, 12, 190 (1964).

2. Solid State Physics. Dr. D. C. Rich, Professor of Physics.

During the current contract period, work on the properties of metals has continued using magnetoacoustic techniques. The electronic contribution to the acoustic properties of a medium can be calculated by writing the equation of motion for the medium and solving for the dispersion relation. The basic equation of motion is

$$\rho \frac{d^2 \xi_i}{dt^2} = \partial T_{ij} / x_j \quad (1)$$

where  $\xi_i$  is the elastic displacement and  $T_{ij}$  is the stress tensor. In the absence of phonon-electron interaction,

$$T_{ij} = C_{ijkl} S_{kl} \quad (2)$$

where

$$S_{kl} = \frac{\partial \xi_k}{\partial x_l} \quad (3)$$

is the strain tensor. In the simple case of an isotropic medium the dispersion relation is

$$\omega = ks \quad (4)$$

where

$$s = (c/\rho)^{1/2} \quad (5)$$

is the velocity of the wave.

Electron-phonon interactions are inserted into the equations by appropriately altering the stress-strain relations, eq. (2). Where the electron-phonon coupling is via a deformation potential, eq. (2) has the form (Ref 3)

$$T_{jk} = C_{jklm} S_{lm} - \sum_i n_i C_{jk}^i \quad (6)$$

where  $C_{jk}^i$  is the deformation potential tensor for carriers of type  $i$  and carrier density  $n_i$ .

The equation of motion is then, for a one-dimensional medium,

$$\frac{d^2 \xi}{dt^2} = s^2 \frac{d^2 \xi}{dx^2} - \sum_i C_i \frac{\partial n_i}{\partial x} \quad (7)$$

This can be solved by noting that  $\xi \propto \exp [i(qx - \omega t)]$ , where  $\omega$ ,  $q$  are the frequency and wave number of the sound wave and by setting

$$n_i = n_i^0 + n_i^1 \quad (8)$$

where  $n_i^0$  is the density of carriers in the absence of the sound wave and  $n_i^1$  is a perturbation, also assumed proportional to  $\exp [i(qx - \omega t)]$ . The carrier densities are written in terms of the respective current densities by means of the equations of continuity and the current densities can be related to externally applied electric and magnetic fields by means of constitutive relations derived from manipulation of the Boltzman transport equation. When this complicated process is carried through (ref 1), the desired dispersion relation is obtained for longitudinal waves:

$$\omega^2 = q^2 s^2 \left[ 1 + \frac{iq^2 (C_e + C_p)^2}{2\rho e^2 \omega s^2} \sigma_{||}' \right] \quad (9)$$

where  $\sigma_{||}'$  is an effective conductivity in the direction of propagation and includes effects of external fields. The velocity of sound is the real part of  $\omega/q$ ; this gives for the normalized charge in  $s$  (Ref 2)

$$\frac{\Delta s}{s} = \frac{q^2 (c_e + c_p)^2}{\rho e^2 \omega s^2} \text{Im} \sigma_{||}' \quad (10)$$

During the current reporting period, work has continued on an experiment to measure the velocity of sound of ultrasonic pulses in Bismuth single crystals when  $V_d \sim V_s$ , where  $V_d$  is the drift velocity of conduction electrons and  $V_s$  is the velocity of sound. The theoretically expected behavior is shown in Fig. 1.

The necessary high drift velocity of the electrons in the sample can be established by imposing mutually perpendicular D.C. electric and magnetic fields in the sample. To establish the necessary electric field it is necessary to pass large currents through the sample while limiting power dissipation in the crystal to levels which can be tolerated in an experiment performed in liquid helium necessitates pulsing

these large currents. The pulse generator in Fig. 2 was designed and constructed for this purpose; it will furnish 45 ampere pulses of duration up to 400  $\mu$ sec at repetition rates up to 40 pulses/sec. This current capability is also adequate for ultrasonic amplification experiments, which require  $V_d \gg V_s$ .

All experimental apparatus has been completed; completion of the experiment awaits preparation of a suitable sample. Bismuth single crystals were found difficult to machine on a spark machine; ten of eleven single crystals recrystallized during spark planning. For this reason an acid planning machine has been designed and is now under construction.

A paper on the results to date has been given at the Beaumont, Texas, meeting of the AAPT, March 16, 1968, (ref 4). The results are being incorporated into a M.S. thesis, but publication is being deferred, pending results using better samples.

References

- (1) Cohen, Harrison, Harrison, Phys Rev 117, 937 (1960)
- (2) H. N. Spector, Phys Rev 134, A507 (1964)
- (3) H. N. Spector, Solid State Phys 19, 291 (1966), Academic Press, New York
- (4) N. P. Thiessen and D. C. Rich, "Effects of External Electric and Magnetic Fields on Velocity of Sound in Bismuth," AAPT Meeting, March 16, 1968, Beaumont, Texas

### 3. Atomic Physics. Dr. R. H. Walker, Associate Professor of Physics.

#### a) Spin-Dependent Atomic Collisions (B. W. Mayes and C. K. Chang)

A theory of angular momentum transfer in the collision of simple atomic systems was formulated. This theory was used to determine various spin transition cross-section including those for spin exchange and hyperfine transitions. At the present time this treatment has been applied only to collisions involving identical alkali atoms. Results have been obtained for hydrogen, lithium, sodium, potassium, rubidium, and cesium. The calculations were carried out for a sufficient range of kinetic energies in each case to allow thermal averages and hence results which can be compared directly with experimental results. This comparison is quite good, perhaps better than one should expect. An exception is claimed for our results on hydrogen-hydrogen collisions. In this case, the possible processes are sufficiently well known, and the calculations were performed in such a way so that our result should be quite good, probably better in fact than the experimental results.

The above work has resulted in one Ph.D. thesis and one M.S. thesis. In addition two papers were presented at the January, 1967 meeting of the American Physical Society. Abstracts of the papers (published in the Bulletin of the American Physics Society) are given below.

Spin-Exchange Cross Sections in Atomic Hydrogen. B. W. Mayes, II (introduced by R. H. Walker) and R. H. Walker, University of Houston. The formalism developed by Glassgold<sup>1</sup> for calculating cross sections for collisions between alkali-like atoms in which angular momentum is transferred is used to calculate spin-exchange cross sections for atomic H in the ground state. The kinetic energies for which the treatment is valid are limited from above by the Born-Oppenheimer approximation and from below by the assumed degeneracy of the hyperfine states. At large internuclear separations the Pauling-Beach<sup>2</sup> interaction is used as a potential for both the  $S = 0$  and the  $S = 1$  states. For separations less than 0.8 Bohr radii, the potentials in both states are from a molecular orbital calculation; while at intermediate separations the potentials come from a variational treatment<sup>3</sup> and from 2nd-order perturbation theory.<sup>4</sup> In particular, total unpolarized scattering cross sections and cross sections for the hyperfine transition  $f = 1$   $f = 0$  are calculated with and without consideration of the effect of identical particles.

Spin-Exchange Cross Sections of Alkali Atoms. C. K. Chang (introduced by R. H. Walker) and R. H. Walker, University of Houston. In the

collision of alkali-like atoms, an important feature of the process is the exchange of electrons between the two colliding atoms. To calculate numerically spin-exchange cross sections, the spin-dependent interaction characterizing the scattering is required. This interaction for two alkaline atoms is calculated by individually considering the interactions due to the valence S electrons and to the closed electronic shells of the two atoms. The valence S-electron interaction is generated phenomenologically from the known H-H inter-atomic potential and the closed-shell interaction from interatomic potentials of inert atoms corresponding to the cores. These potentials so obtained are in agreement with those constructed from band spectra. Six different cross sections were calculated by semiclassical techniques and by partial wave analysis for each of the six alkaline atomic systems H, Li, Na, K, Rb, and Cs, for 124 different relative kinetic energies. These cross sections are finally averaged thermally. The results obtained by partial wave analysis agree rather well with experiment. Comparison of the results of the two methods are too small by about 10% for the heavier atoms and by about 50% for low-energy H and Li atoms.

#### b) Perturbations in an Electron Gas. (John Paulsel)

The specific problem which has been considered is the determination of that critical density of an electron gas for which an unscreened perturbation will produce a localized state of zero energy. A solution of this problem will give information as to whether a given impurity will produce trapping states in a given metal. Our original approach has turned out to be unsatisfactory. The starting point was to assume that the self-consistent potential resulting from the electron gas did in fact bind an electron. A hydrogen like wave function was assumed with a variational parameter and the self-consistent potential determined in terms of this parameter. The total energy was then calculated and the condition of minimum energy obtained. This energy was then considered as a function of electron density with the hope of finding that density which yields zero energy. It was found that the dependence of energy upon density was such that the energy vanished only asymptotically with decreasing density. It appears that the above scheme cannot be made self-consistent or that the perturbation treatment was not carried out to sufficiently high order. We have therefore adopted a different approach, namely that of propagator theory.

Currently, we are attempting to construct the propagator for the system including the effects due to the perturbation. We shall attempt to find the required propagator by Feynman's selective summation technique. Once this is determined, the singularities of the full propagator determine the eigen values of the total hamiltonian. The

existence of a discrete pole will then yield the desired information. A meaningful start on this approach is just now getting under way. It is expected that at least six months will be required for this formulation of the problem.

c) Metallic Lattice Dispersion Relations. (Gilbert Hopkins)

A model for a metal has been adopted in terms of which lattice dispersion relations can be obtained with only one parameter which is undetermined. This model may be contrasted with the usual force constant approach in which there are as many undetermined constants as there are atoms which interact with a given atom. This number is quite large in the case of metals due to the long range screening of the conduction electron which arises from the existence of a sharp Fermi surface. We have approached the problem by treating the electron screening by perturbation theory which directly takes into account the long range interactions. The result is a secular equation whose roots yield the lattice vibration spectrum and whose eigen values yield the accompanying polarization for that mode. The elements of the secular determinant are extremely complicated quantities and have required extensive numerical calculation for their evaluation. The one undetermined parameter is the range for a short range ion-ion interaction whose value could in principle be determined. We have chosen to choose that value which gives optimal agreement with the experimental information available.

Extensive calculations have been carried out for the metals Al and Pb with the result that our dispersion curves agree very well with the results of neutron scattering experiments over the whole Brillouin zone, in many cases to within experimental uncertainty. We are in the process of applying the theory to the alkali metals and to copper.

Our calculations to date are such that the best agreement is obtained at low frequencies and poorer agreement at high frequencies, particularly for the transverse modes. The model is such that this should be so and can be corrected by the inclusion of magnetic effects which become appreciable at higher frequencies. The necessary modification of the theory to include these effects are being formulated and will shortly be applied to the metals indicated above.

Once dispersion curves are obtained, many macroscopic parameters can be calculated. These include the speed of acoustic waves in various directions, the macroscopic elastic constants, and various thermal properties. The former of these will be evaluated presently and compared with experiment. Crucial to the determination of thermal

properties is the phonon density of states which can be found from the calculated dispersion curves. The evaluation of the density of states offers perhaps the most sensitive test of the theory since the density of states depends not only upon the values of the frequencies at various wavelengths but also upon the slope of the dispersion curve. Incoherent neutron scattering experiments yield large peaks in the phonon density of states for certain frequencies. The positions of these peaks calculated from our results will be a crucial test of the model we have assumed.

The work discussed here will result in one M.S. thesis expected to be completed by the end of this summer and at least one publishable paper.

d) Low Temperature Thermal Properties of Rotating Crystals. (Kan Fong)

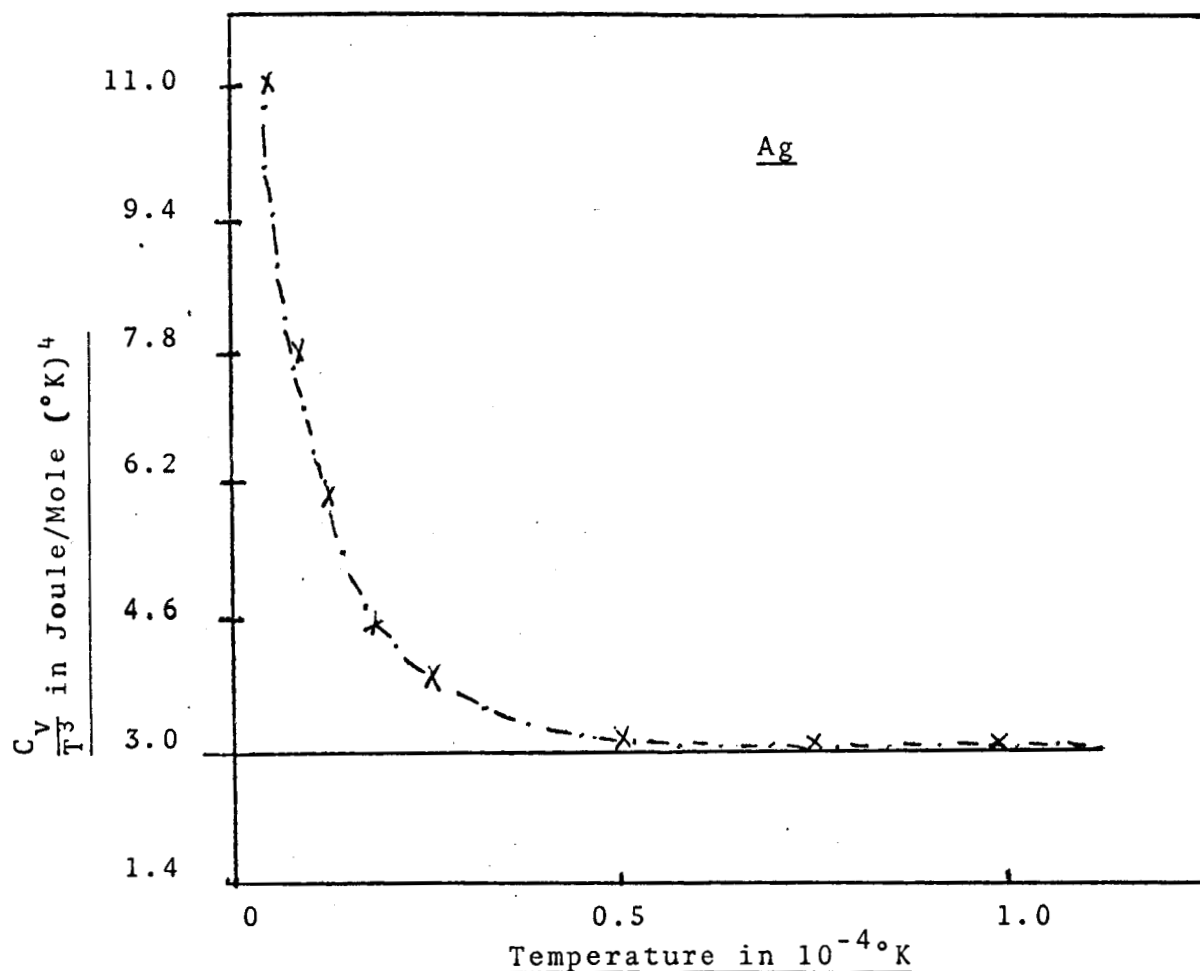
Inspection shows that the respective hamiltonians for a lattice of charges in a weak external magnetic field and a lattice of mass points under rotation are formally identical. This suggests a rotational analogue of magnetic effects at low temperature such as adiabatic demagnetization. That such effects should exist at low temperatures is obvious since a little reflection shows that those modes of frequencies less than the rotational frequency are effectively frozen out and hence do not contribute to the specific heat. Competing effects of the same order of magnitude makes an estimate of the change in specific heat difficult. One can show, however, that the form of the temperature dependence is

$$C_v = C_0 \left(\frac{T}{\theta}\right)^3 F(T)$$

where  $F(T) = 1$  in the absence of rotation. The problem under study by us is the numerical calculation of this function. Its departure from unity is a measure of the magnitude of thermal effects arising from rotation.

Since only the low temperature region is of interest, the continuum-long wave length approximation is appropriate. The crystal under investigation is then characterized by the macroscopic elastic constants  $C_{ij}$ . The secular equation appropriate for a rotating crystal is obtained from which the vibrational spectrum is determined. The required thermal parameters involve sums over lattice modes which can be approximated by integrals in the standard way. The crystals currently under investigation are of cubic symmetry which is distorted to tetragonal by the rotation. This symmetry is reflected in the vibrational spectra which allows expansion into tetragonal harmonics and the reduction of the required integrals involved to a manageable number.

Calculations have been carried out on a number of crystals. Typical results are indicated below which show the dependence of the specific heat of Ag upon temperature for a fixed rotational angular velocity.



The broken curve gives  $C_v/T^3$  for  $\Omega = 2\pi \times 10^6/\text{sec}$ , while the solid curve gives  $C_v/T^3$  for no rotation.

The results show that at sufficiently low temperatures, the specific heat increases with rotation. Indeed the rotational analogue of adiabatic demagnetization exists. At sufficiently low temperatures, if a crystal is set into rotation by non-dissipative forces, its temperature will decrease. The magnitude of the rotation velocity required to produce changes in heat capacity at attainable temperatures seems

to make practical application of this phenomenon doubtful.

As part of the calculations required for the specific heat, the effective Deby temperatures for various metals have been obtained. The agreement with experimental values is quite good which is an affirmative check on the numerical procedures used. The work carried out on this project will result in one M.S. thesis which will be completed by the end of this summer.

#### References

- (1) A. E. Glassgold, Phys Rev 132, 2144 (1963)
- (2) L. Pauling and J. Y. Beach, Phys Rev 47, 686 (1935)
- (3) W. Kolos and C. C. J. Roothan, Rev Mod Phys 32, 219 (1960)
- (4) A. Dalgarno and N. Lynn, Proc Phys Soc (London) A69, 821 (1956)

4. Cometary Physics, N. S. Kovar, Assistant Professor of Physics.

a) Optical Pumping and the D Line Ratio of Comet 1962 III.  
N. S. Kovar and R. P. Kovar.

Spectral observations of Comet 1962 III made prior to perihelion passage revealed a sodium D line ratio of 2.5. Due to the inadequacy of normal atomic processes in explaining this ratio, an optical pumping process is considered. It is found that such a mechanism can produce the observed D line ratio if the sodium atoms within the coma were under the influence of a magnetic field and if they were excited by circularly polarized radiation from the sun.

This paper has appeared in the April 1968 issue of Solar Physics. A copy of this paper appears in the preceding semi-annual progress report for this grant.

b) Cometary Plasmas and the Solar Wind, M. E. Shelby.

The interaction between a comet and the solar wind has been treated extensively in the literature. Solution of the general flow problem, for example, has been considered by Ioffe (1966), Kovar and Kern (1966), and Biermann, Brosowski, and Schmidt (1967) among others. The general approach in these treatments has been that of gas dynamics. Both a shock front (on the sunward side of the comet) and a contact discontinuity are thought to form.

In the present treatment, for the region interior to the contact discontinuity, an alternate approach is taken. Namely, the assumption is made that the ions moving away from the comet's nucleus are non-interacting and that these ions are specularly reflected back into the region bounded by the contact discontinuity by the solar wind's frozen-in magnetic field. A model is developed which predicts the size and shape of the contact discontinuity and the density of plasma interior to it. Results of this model agree well with observational data.

This research is incorporated in a M.S. thesis to be published in June 1968 and is being prepared for publication in a journal.

c) Atmospheric Refraction and the Gegenschein, H. Schmidt.

Calculations of the effects of the refraction of sunlight through the earth's atmosphere on the intensity of light backscattered from interplanetary dust in the antisolar direction have been performed. It is found that the refraction enhances the intensity of backscattered light by three percent in the antisolar direction. The treatment involves programming of the refraction through a standard atmosphere and Mie scattering of the total refracted and incident light intensity through arbitrary angles. A uniform spatial

distribution of interplanetary dust particles is assumed, with size to wavelength ratios that satisfy a power law distribution function. No account is taken of possible mechanisms for concentrating dust in the region antisolar to the earth. The contribution of refracted light found is small, but may be susceptible to experimental measurement. It cannot explain existing discrepancies between theory and measurement. This work is incorporated in a M.S. thesis to be published in June 1968, and is being examined for publishable content.

5. Space Related Flow Problems, Dr. R. M. Kiehn and Dr. J. W. Kern, Associate Professors of Physics.

a) Applications of Differential Forms. J. Pierce and R. M. Kiehn.

Most of the early work in the theory of differential forms appears in the French literature, and in many works (in French) of Elie Cartan. Applications of the theory to problems in fluid flow and problems in continuous media are very sparse, especially in English. Cartan's works not only contain the original ideas of the theory, but they also contain scattered applications to physical problems.

A first translation of Cartan's "Lectures on Integral Invariants" has been completed during this reporting period. The translation of "Exterior Differential Systems and Their Geometric Applications" is in progress. These works have been prepared for publication, the first translation being currently under review by Academic Press.

(J. Pierce, R. Borochoff, R. M. Kiehn) A weekly seminar in "Applications of Differential Forms" was started in the fall semester of 1967 at the University of Houston. Topics of discussion include Hamiltonian systems and trajectory mechanics. One of the objectives of this seminar is to extend the knowledge of solution trajectories on non-simply connected manifolds.

The application of these methods to problems in trajectory mechanics, fluid dynamics, and electrodynamics will form the first portion of the Ph.D. thesis of J. Pierce.

A second outcome of the seminars has been the development of the idea that gravitation, or acceleration fields, may influence the polarization of electromagnetic signals. A modification of the Sagnac experiment, using a ring-laser, is being studied in order to determine the practicality of measuring the effect of accelerations on the polarization of light by terrestrial techniques. R. Borochoff

(R. M. Kiehn) A significant development during this reporting period, although stimulated by research in the field of vortex flow, is the field of electrodynamics. The achievements are a result of work initiated during the previous grant period (NASA grant 44-005-022).

The theory of differential forms may be used to express Maxwell's Equations<sup>1</sup> as

There exists a one form,  $a$ . (1)

The derived two form  $F = da$ , is harmonic (2)

The importance of such equations does not reside solely with the fact that they are equivalent to the Maxwell's relations in a four-parameter frame; more importantly, they are form statements and if true in one frame, they are true in any other frame of reference linked to the first by means of a smooth, though not necessarily invertible map.

Such a notion extends the Einstein idea that the laws of nature should be true in any reference system, whether related to inertial frames by means of a tensor, invertible, transformation, or not.

Equations (3) and (4) imply that, counter to many implications in the literature, Maxwell's equations are naturally covariant in any frame of reference, whether induced by a Lorentz transformation, or a Galilean transformation. A paper demonstrating the explicit covariance of Maxwell's equations with respect to both Galilean or Lorentz transformations is in preparation. Such a result raises the question as to why the Lorentz transformations are of such fundamental importance in physics. The credence given to the physical validity of the Lorentz transformation, which is often based upon the covariance of Maxwell's equations with respect to Lorentz transformations, must be re-examined.

The answer to this question can be obtained by studying the characteristics of Maxwell's equations. By the use of the theory of forms, the characteristics,  $\phi$ , of Maxwell's equations can be cast into the form:

$$\phi \wedge F = 0 \quad (3)$$

$$\phi \wedge *F = 0 \quad (4)$$

As these are form statements they are again naturally covariant in any frame of reference. However, the equations for the characteristics may be written in the form

$$(\text{grad } \phi)^2 - \frac{(D \cdot B)}{(E \cdot H)} \frac{(\partial \phi)^2}{\partial t} = \frac{(\text{grad } \phi \cdot E)(\text{grad } \phi \cdot H)}{(E \cdot H)} \quad (5)$$

Such an equation is invariant for only the Lorentz transformation. Evidently when we make a physical measurement by means of electromagnetic signals, we detect the characteristic surfaces of Maxwell's equations. The characteristic surfaces are the only surfaces upon which the field quantities or their derivatives may be discontinuous. The equations of the characteristics, being sums of squares with constant coefficients, (assuming that the RHS of (5) vanishes) are invariant only with respect to Lorentz transformations.

b) Computer Techniques. J. Shores and J. Pels, and R. M. Kiehn.

The machine code for the piecewise potential theory\* has been modified to accept periodic and ring boundary conditions. Test problems for 3-fold and 6-fold ring symmetry systems have been attempted. The algebraic formulation of non-analytic boundary conditions is under investigation. It has been established that the criteria, continuity of slope and continuity of value, preserve quantum mechanical probability and probability current. On the other hand, continuity of current and probability do not require continuity of state function slope and value. Therefore, there exists the possibility that discontinuous non-analytic solutions to the Schroedinger equation may exist, and may have physical significance. This work is the basis of the M.S. thesis of J. Shores.

Analysis of scattering problems indicate that non-analytic solutions may be connected to the notion of complex quantum mechanical potentials. The inclusion of complex potentials has led to investigation of "Normal" operators in Quantum Theory, which permit the formulation of complex, not necessarily, hermitean interactions. The modifications of quantum theory required to admit Normal rather than Unitary operators forms the basis of the M.S. thesis of J. Pels. The study of the solutions to the Schroedinger central field problem which are not analytic (but which are bounded and quadratically integrable) forms the basis of the M.S. thesis of R. Arlen.

c) Non-Linear Source Terms in Electrodynamics. J. Shores and R. M. Kiehn

The methods of continuous analytic continuation<sup>2</sup> have been formulated into a computer program to solve the non-linear, second order, differential equation of the form:

$$\nabla^2 \phi = a + b\phi + c\phi^2 + d\phi^3. \quad (1)$$

Such an equation is of interest from an academic point of view as the generator of elliptic functions, and also from the theoretical physics point of view, as the descriptive equation for self-consistent charge distributions. In particular, the equation

$$\nabla^2 \phi = \phi - \phi^3 \quad (2)$$

under certain circumstances can be interpreted, in terms of Maxwell's equations and an equation of state, as an equation representing an elementary charged object.<sup>3</sup>

The most significant result of studying such equations by means

of machine techniques is the fact that the solutions to this non-linear equation appear to contain a discrete set, which are bounded in an integral sense. The asymptotic solutions to equation (2) are the values  $\pm 1$ , and 0. Machine studies indicate that the solutions asymptotic to zero seem to form a discrete set. Those discrete, bounded, solutions which are symmetric about the origin are characterized by a sequence of different amplitudes at the origin; they form a sequence of solutions with increasing numbers of nodal points which is strongly suggestive of some eigen quality for this non-linear differential equation. The first seven discrete modes have been found by exploratory numerical analysis.

The detection of such discrete solutions was aided by the incorporation of a SC-4020 plot routine into the continuous analytic continuation code. The code package was made available to the NASA-MS. A summary report is being prepared for publication by J. Shores.

d) Solar-Wind Termination and the Interstellar Medium, J. W. Kern and C. L. Semar.

The formulation of a gas dynamic flow with a distributed mass source was examined. The equation of motion of the medium was constructed, and the correct energy conservation equation for the flow was obtained. It is found that for nearly all situations of physical interest (flow of the solar wind in the vicinity of a comet, flow of the solar wind into the interstellar medium, general hydromagnetic flows in the presence of stationary neutrals, etc.), the kinetic energy density of the flow has an additional source term. That is, the usual relation between pressure and the flow volume element no longer applies. This means that the solutions obtained previously by many workers to problems of this kind are invalid. The results are being applied to the problem of the termination of the solar wind in the interstellar medium, and to the problem of the flow of solar wind past a comet nucleus. A portion of this work was supported under the MSC Solar Physics Grant 44-005-041. A paper reporting on the work on the solar wind termination problem was given at the 1968 National Meeting of the American Geophysical Union, April 8-12, Washington D.C., is being incorporated in a M.S. thesis, and prepared for publication in the Journal of Geophysical Research.

References

- (1) "Exterior Forms and Electrodynamics", R. M. Kiehn presented at the Austin meeting of the A.P.S., February, 1967.
- (2) H. T. Davis, "Introduction to Non-Linear Differential and Integral Equations, #7 U.S.A.E.C. (1962).
- (3) R. M. Kiehn, "Poincare Stresses and Mach's Principle." Bull. A.P.S. 11, 773, (1966).

# THE PHYSICS OF FLUIDS

VOLUME 11, NUMBER 3

MARCH 1968

## Pressure Measurements in Subcritical Pure Superfluid Helium Flow

HENRY E. CORKE AND ALVIN F. HILDEBRANDT

*Department of Physics, University of Houston, Houston, Texas*

(Received 25 September 1967)

The measurement of pressure in He II with flowing superfluid superimposed in a stationary normal fluid was undertaken to demonstrate ideal fluid character of the superfluid below critical velocities. Quantitative agreement with Euler's equation with zero curl is shown with slip-flow boundary conditions. Thus, Bernoulli's equation holds for potential flow and superfluid accelerations occur without dissipation. The method of pressure measurement demonstrates that net forces on an object in non-uniform potential flow can be measured.

### I. INTRODUCTION

Pellam and Hanson<sup>1</sup> studied the torques on a Rayleigh disc in a He II second sound field. The results indicated that both the superfluid and normal fluid simultaneously produced torques on the disc via the average Bernoulli pressure. The alternative nature of the flow, the interplay of the two fluids, and the probable critical-peak velocities about the disc are features avoided in the work reported here. Craig and Pellam's<sup>2</sup> studies of lift on airfoil surfaces demonstrated that pure superfluid flow is potential in nature, and that any object in uniform subcritical superfluid flow will experience no net forces. Pressure measuring techniques utilizing the Venturi tube or Pitot tube are useless for potential flow, as seen for example in Ref. 3. This failure has recently been elucidated by Meservey,<sup>4</sup> who considered the potential solution for the velocity in the Venturi tube. However, pressure gradients about an object in nonuniform potential flow without circulation can produce net forces, and this fact was utilized here to measure pressures in superfluid helium for steady-state and constant-acceleration conditions.

The ideal-fluid character of superfluid has been expounded by many authors; recently Anderson<sup>5</sup>

utilized a quantum mechanical approach to also reach this conclusion. Through the concept of a superfluid order parameter, he has pointed out that the time rate of change of the phase factor  $\phi$  of the order parameter is proportional to the chemical potential  $\mu$ :

$$\hbar \frac{d\phi}{dt} = \mu. \quad (1)$$

With  $\phi$  as a thermodynamic variable, in the steady state the chemical potential must be constant everywhere as in Bernoulli's equation for potential flow. The result of taking the gradient of (1) and making the identification  $\hbar \nabla \phi = mv$ , according to Anderson, has two interpretations. One is related to phase slippage by quantized vortex motion, which is not under consideration here. The other, since the result leads to Euler's equation, is frictionless acceleration. The supposition is that a chemical potential difference between elements of the superfluid will produce continuous acceleration without frictional damping.

### II. APPARATUS

Nonuniform flow was produced by pumping superfluid via the fountain effect, radially inward between two flat circular pyrex plates, with opposing surfaces flat to within  $10^{-4}$  cm (Fig. 1). The thermomechanical pump assembly utilized a closely packed jewelers-rouge semipermeable barrier A to prevent normal fluid flow. To eliminate thermal conduction

<sup>1</sup> J. R. Pellam and W. B. Hanson, *Phys. Rev.* **85**, 216 (1952).

<sup>2</sup> P. P. Craig and J. R. Pellam, *Phys. Rev.* **108**, 1109 (1957).

<sup>3</sup> R. Bowers and K. Mendelssohn, *Proc. Roy. Soc. A* **213**, 158 (1952).

<sup>4</sup> R. Meservey, *Phys. Fluids* **8**, 1209 (1965).

<sup>5</sup> P. W. Anderson, *Rev. Mod. Phys.* **38**, 298 (1966).

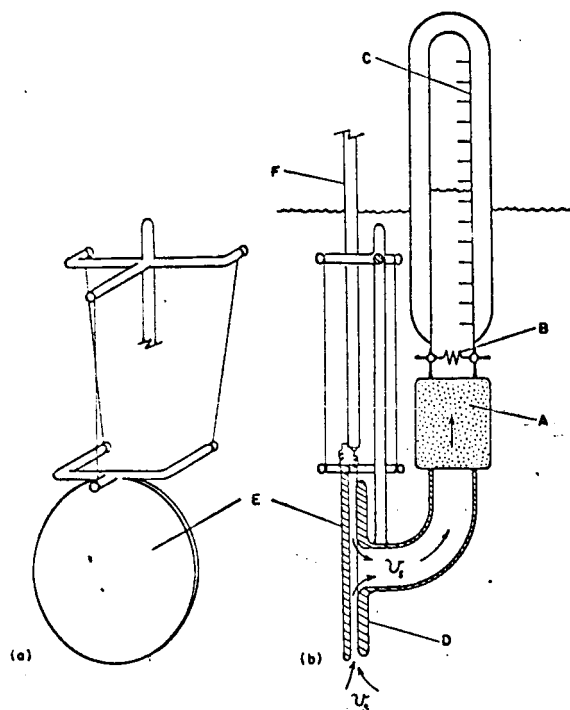


FIG. 1. (a) Perspective view of the trifilar pendulum plate support configuration. The pendulum has an effective length of 6.7 cm and a mass of 5.4 g. (b) Schematic of the thermomechanical pump and pendulum-plate capacitor with coax probe connections. The inner and outer radii of the annular plate D are 0.79 and 1.85 cm, respectively.

along the barrier it was made 3 cm long and encased in a thin-walled copper cylinder. Thus, extraneous normal and superfluid currents between the plates were inconsequential. Direct current in the heater B caused the helium level to rise in the vacuum jacketed milliliter graduate C. From the rate of rise the volume flow rate was determined.

Circular plate E was supported as a trifilar pendulum with three hinged 0.001-in. wires, and aligned to maintain parallel orientation with respect to the annular plate D. The opposing surfaces of the plates were coated with conductive material and electrically connected as a capacitor, via coax probe F, to an  $L$ - $C$  tuned Franklin oscillator. The frequency of the oscillator was detected with a digital frequency counter, and the significant digits were recorded in analog form with a  $y$ - $t$  plotter. Thus, displacements of the pendulum due to pressure gradients were recorded as frequency changes. Pendulum plate separations from 0.006–0.02 cm were selected by external tilting of the experiment in a plane perpendicular to the annular plate surface and determined by the oscillator frequency. Due to the pendulum suspension, (a) in Fig. 1, tilting the experiment in a plane parallel to the annular plate surface caused

a slight rotation of the pendulum plate about the vertical. With a set plate separation this rotation altered the capacitance about a minimum. Hence, horizontal parallel-plate alignment was obtained by minimizing the capacitance which was observed by a frequency maximum. Vertical parallel alignment of the plates was adjusted during assembly.

Frequency-capacitance calibration was performed over a frequency range of 7–15 MHz. With fixed capacitance the oscillator stability was better than one part in  $10^6$  for periods of 3–4 min. This stability along with the inherent damping of the pendulum in He II, while closely juxtaposed to the annular plate, made it possible to measure millidyne forces to an accuracy of better than 10%. Calibration of the forces to displace the pendulum was performed by applying known voltages through a high impedance to the pendulum plate capacitor while recording the frequency change. From each value of voltage and corresponding capacitance the displacement force was calculated and related to the change in frequency. Forces required to displace the pendulum were also calculated from the known length and mass of the pendulum but ignoring the spring constant of the coax probe connecting wire. These estimates resulted in values roughly 15% lower than those by the calibration technique.

### III. CALCULATIONS

In the annular region between the plates the flowing superfluid superimposed in the stationary normal fluid was considered incompressible, therefore  $\nabla \cdot \mathbf{v} = 0$ . With the condition of potential flow ( $\text{curl } \mathbf{v} = 0$ ), Euler's equation was used to describe the motion of the superfluid, where the density was that of the superfluid component

$$-\nabla P = \frac{1}{2} \rho_s \nabla v_s^2 + \rho_s \frac{\partial \mathbf{v}_s}{\partial t} \quad (2)$$

The velocity profile was found as a solution of Laplace's equation, with the boundary condition that  $\nabla \Phi$  or  $\mathbf{v}_s$  was everywhere tangential to the surface.  $\mathbf{v}_s$  outside the narrow annular region was negligible and set equal to zero; and since the edges of the plates were rounded with a radius of curvature greater than or equal to that of the channel width the velocity was considered uniform near the plate edges. These criteria have been demonstrated earlier by Hildebrandt *et al.*<sup>6</sup> in an analogous potential problem dealing with magnetic fields in superconducting shells. The superfluid velocity profile was

\* A. F. Hildebrandt, H. Wahlquist, and D. D. Elleman, J. Appl. Phys. 33, 1798 (1962).

FIG. 2  
frequency  
plate as  
accelera  
maintain  
constant  
flow 0.1

thus co  
nular r  
the rad

where  
capacit  
in the  
pressur  
by inte

$P = -$

$\dot{V}$  is t  
 $r_2$  is t  
first te  
third t  
annula  
sary fo  
critical  
annula  
be nee  
pendul  
the pre

The fr  
the acc  
annula

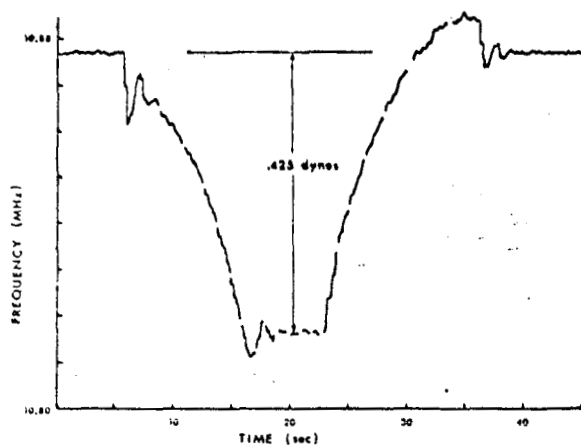


Fig. 2. Example of the  $y$ - $t$  plotter record showing the frequency decrease due to the displacement of the pendulum plate as the result of superfluid flow. At 6 sec constant accelerated flow was started, after 17 sec steady flow was maintained, until at 23 sec the flow was decelerated at a constant rate. The breaks in the trace indicate the time to flow 0.1 of a ml of superfluid.

thus considered flat across the channel in the annular region. The resulting velocity is a function of the radial distance  $r$ :

$$v_r = \frac{\rho \dot{V}}{2\pi \rho_s D r}, \quad (3)$$

where  $D$  is the plate separation determined from the capacitance, and  $\dot{V}$  the measured-volume flow rate in the milliliter graduate. The expected change in pressure on the pendulum plate was then evaluated by integrating Euler's equation over  $r$ :

$$P = -\frac{\rho^2 \dot{V}^2}{8\pi^2 \rho_s D^2 r^2} + \frac{\rho \dot{V}}{2\pi D} (\ln r - \ln r_2) + P_i, \quad (4)$$

$\dot{V}$  is the rate of change of volume flow rate, and  $r_2$  is the outer radius of the annular region. The first term is the Bernoulli pressure, the second and third terms the pressure changes occurring in the annular channel and the inner central region necessary for the acceleration of the superfluid. Above critical velocity with dissipation occurring in the annular channel an additional pressure term would be needed to describe the flow. The force on the pendulum plate was then calculated by integrating the pressure over the area of the plate:

$$F = \frac{\rho^2 \dot{V}^2 \ln(r_2/r_1)}{4\pi \rho_s D^2} + \frac{\rho \dot{V} A}{4\pi D}. \quad (5)$$

The first term is the Bernoulli force  $F_B$ , the second the acceleration force  $F_A$ , where  $A$  is the area of the annular plate.

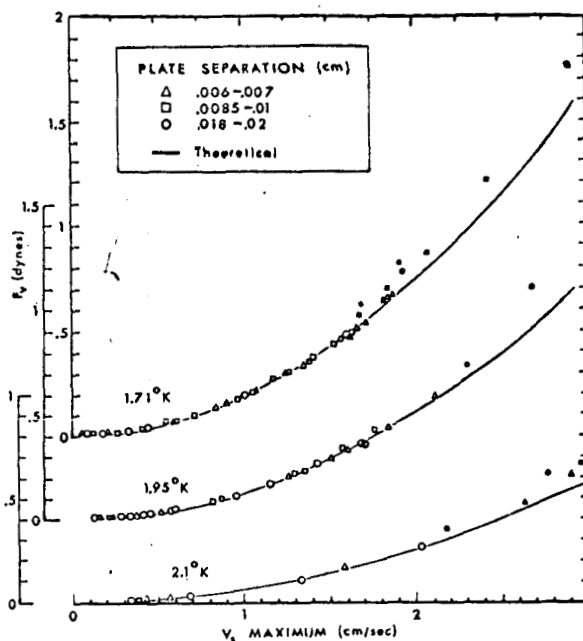


Fig. 3. Plot of the measured forces due to superfluid flow versus the maximum velocity. The solid lines are calculated from Bernoulli's equation at each temperature. Solid points on the graph indicate that the superfluid flow has exceeded critical velocity which is interpreted as an additional force on the pendulum plate.

Quantitative data for two types of flow have been obtained; steady state ( $F_A = 0$ ), and constant acceleration ( $F_A = \text{const}$ ). To produce constant acceleration the power in the thermomechanical pump heater must change linearly in time, so the current time. Figure 2 is a typical  $y$ - $t$  plotter record of the change in frequency due to forces on the pendulum versus time. At the left the current in the heater was turned on and increased as the square root of time. The constant acceleration force was immediately present along with the increasing Bernoulli force. In the center the current was held constant for steady state where only the Bernoulli force was present. On the right the current was decreased as the square root of time which reversed the acceleration force, and at low velocities the pendulum was displaced to the other side of the zero force position. The procedure took less than 60 sec, while observation of the helium level passing each 0.1-ml mark on the graduate scale was indicated by momentarily lifting the recording pen. From this data the volume flow rate  $\dot{V}$  and the rate of change of volume flow rate  $\dot{\dot{V}}$  were determined to compute the theoretical forces. The measured forces  $F$ , were determined at various points of the  $y$ - $t$  curve from the change in frequency and the displacement force calibration data.

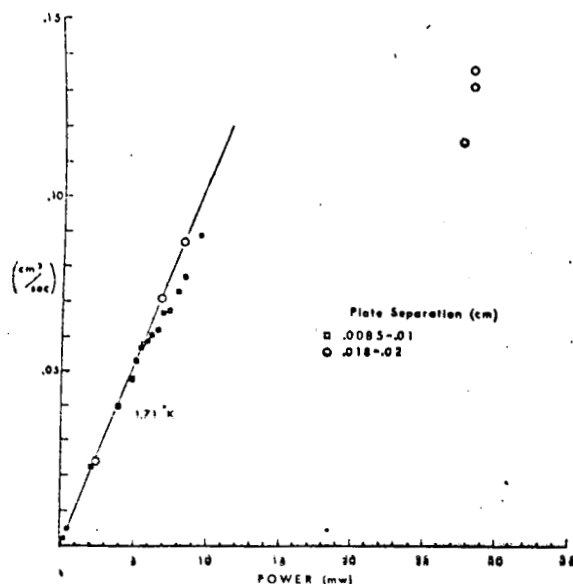


FIG. 4. Two examples of volume flow rate data as a function of power input to the thermomechanical pump heater. The points at higher flow rates which fall below the linear portion of the curve indicate dissipative losses in the flow as the result of exceeding superfluid critical velocity.

#### IV. DATA

Figure 3 is the steady-state force data plotted as a function of maximum velocity (this occurred at the inner radius  $r_1$ ) for the indicated temperatures and plate separations. The theoretical Bernoulli force (solid line) is shown for comparison. Since the ratio of measured force to Bernoulli force  $F_m/F_B$  was independent of the value of the plate capacitance, it was estimated a comparison of the two forces should not deviate by more than 7%. Above about 0.1 cm/sec agreement with the Bernoulli force was excellent until at the higher velocities a critical value was reached. This produced an additional pressure gradient along the annular channel due to the onset of dissipation. To confirm this, volume flow rate data were plotted versus heater input power. It can be seen in Fig. 4 there is a linear relationship for the smaller volume flow rates followed by a decrease in slope for higher velocities. A departure from linearity indicates that the superfluid critical velocity has been exceeded.<sup>7</sup> Force measurements for which departure from linearity of the flow rate versus power were observed are noted as solid points in Fig. 3. The increased force due to dissipation, while maintaining constant flow rate, appeared as a gradual force build up of duration on

<sup>7</sup> P. L. Kapitza, J. Phys. 4, 181 (1941).

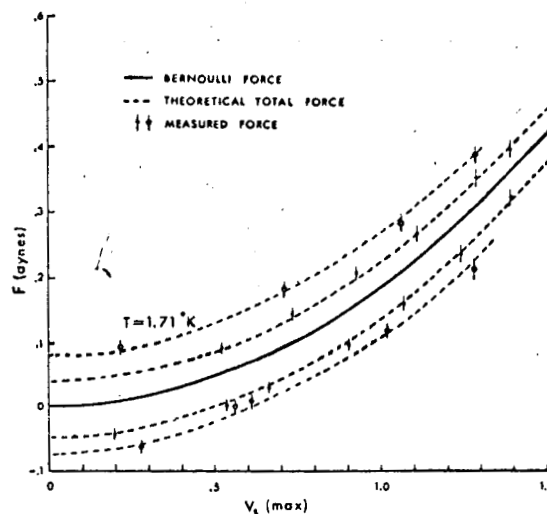


FIG. 5. Forces as a function of maximum velocity with constant superfluid acceleration. The top broken lines are calculated for accelerations of 0.118 and 0.172 cm/sec<sup>2</sup>, the lower broken lines for decelerations of 0.123 and 0.16 cm/sec<sup>2</sup>. The force  $F_A$  to accelerate the superfluid is the difference between the total force (broken line) and the Bernoulli force (solid line). Coincidence of the measured forces with the calculated forces indicates the absence of dissipation.

the order of 5-10 sec. This might be explained by a gradual increase of vortex lines in the annular channel and or the spreading of the vortex lines radially outward from the inner radius at the highest velocity region. This is based on the assumption that the growth of turbulence is similar to that reported by Mendelssohn and Steele<sup>8</sup> with heat currents in wide channels. Further investigations into the area of dissipation are being carried out with the present device. Precise values of critical velocities were not determined but the observed range of 1.5-2 cm/sec, dependent upon plate separation and temperature, is in agreement with other experimental observations.

Constant acceleration data is shown in Fig. 5 as a function of maximum velocity. The Bernoulli force is indicated by the solid line, and the broken lines include both the Bernoulli and the acceleration forces as calculated from the volume flow rate and rate of change of volume flow rate. Two different accelerations (upper lines) and decelerations (lower lines) are presented for 1.71°K. The measured forces with estimated uncertainty are in good agreement with the calculations indicating that no additional forces such as those due to dissipation were present.

<sup>8</sup> K. Mendelssohn and W. A. Steele, Proc. Phys. Soc. 73, 144 (1959).

## V. CONCLUSIONS

The nonuniform circulation-free superfluid flow about the pendulum plate produced net forces which quantitatively agree with the classical fluid equations to within the accuracy of the experiment. Thus, the slip boundary condition must be correct at least to within the order of  $10^{-4}$  cm. Superfluid undergoing constant acceleration experienced no dissipative losses and under the influence of a chemical poten-

tial gradient accelerated freely until reaching critical velocity.

## ACKNOWLEDGMENTS

This work was partially supported by National Aeronautics and Space Administration Grant NGR 44-005-022. One of us (H. E. C.) was a National Aeronautics and Space Administration Trainee under Grant NsG(T)-52#1.